Research Square

Preprints are preliminary reports that have not undergone peer review.
They should not be considered conclusive, used to inform clinical practice,
or referenced by the media as validated information.

Visible–Near Infrared Spectroscopy for Nondestructive Prediction of Firmness and Moisture Content in Bronzing-Affected Jackfruit (Artocarpus heterophyllus cv. ‘Tekam Yellow’)

Kok Jeng Lim

limkokjeng@gmail.com

Universiti Putra Malaysia

Phebe Ding

Universiti Putra Malaysia

Nazmi Mat Nawi

Universiti Putra Malaysia

Mashitah Jusoh

Universiti Putra Malaysia

Research Article

Keywords: Jackfruit (Artocarpus heterophyllus), bronzing disorder, visible near infrared spectroscopy (Vis–NIRS), nondestructive quality assessment, firmness prediction, moisture content, partial least squares regression (PLSR)

Posted Date: June 2nd, 2026

DOI: https://doi.org/10.21203/rs.3.rs-9864424/v1

License: This work is licensed under a Creative Commons Attribution 4.0 International License.
Read Full License

Additional Declarations: No competing interests reported.

Visible–Near Infrared Spectroscopy for Nondestructive Prediction of Firmness and Moisture Content in Bronzing-Affected Jackfruit (*Artocarpus heterophyllus* cv. 'Tekam Yellow')

Kok Jeng Lim[1], Phebe Ding[1], Nazmi Mat Nawi[2,3] and Mashitah Jusoh[1]

[1]Department of Crop Science, Faculty of Agriculture, Universiti Putra Malaysia, 43400 UPM Serdang, Selangor Malaysia.

[2]Department of Biological and Agricultural Engineering, Faculty of Engineering, Universiti Putra Malaysia, 43400 UPM Serdang, Selangor, Malaysia.

[3]Institute of Plantation Studies, Universiti Putra Malaysia, 43400 UPM Serdang, Selangor, Malaysia.

Email addresses: : limkokjeng@gmail.com, phebe@upm.edu.my, nazmimat@upm.edu.my, mashitahj@upm.edu.my,

Corresponding Author:

Name: Kok Jeng Lim

Email: limkokjeng@gmail.com

Abstract

The Malaysian jackfruit industry is increasingly threatened by "jackfruit-bronzing," a disease caused by *Pantoea stewartii* subsp. *stewartii*, which manifests as yellowish-orange to reddish discoloration of the pulp while leaving the rind visually unaffected. The cv. 'Tekam Yellow' cultivar is particularly vulnerable, resulting in substantial postharvest losses. This study explores

the feasibility of employing visible near infrared spectroscopy (Vis-NIRS) as a non-destructive method to predict internal bronzing through the estimation of rind or flesh firmness and rind, flesh or seed moisture content. Spectral reflectance data were acquired non-destructively from the rind surface of jackfruit, and the resulting spectra were used to predict rind firmness, and moisture content of rind, flesh, and seed tissues. Jackfruits at 10, 12, and 14 weeks after anthesis (WAA) were analyzed within the 500–950 nm wavelength range. Partial least squares regression (PLSR) models were developed and optimized using preprocessing techniques such as Savitzky–Golay smoothing, standard normal variate (SNV), and multiplicative scatter correction (MSC). The best-performing models yielded high determination coefficients for both calibration (Rc^2) and validation (Rv^2), reaching up to 0.99, with root mean square error of calibration (RMSEC) and validation (RMSEV) values as low as 0.67 N and 0.74% w.b., respectively. Destructive reference measurements were conducted in parallel and analyzed using ANOVA and Fisher's protected least significant difference (FPLSD) test at $p \leq 0.05$. Results demonstrated that Vis–NIRS applied through the rind surface provided reliable prediction of firmness and moisture-related attributes associated with internal bronzing disorder in jackfruit. The developed approach shows strong potential as a rapid and non-invasive technique for early bronzing detection and postharvest quality assessment in jackfruit.

Keywords: Jackfruit (*Artocarpus heterophyllus*), bronzing disorder, visible near infrared spectroscopy (Vis–NIRS), nondestructive quality assessment, firmness prediction, moisture content, partial least squares regression (PLSR)

1 Introduction

Jackfruit is a widely cultivated tropical fruit in Southeast Asia, known for its high nutritional value and economic significance. Its large fruit size (10–25 kg), coupled with multiple ends uses—including consumption of the flesh, utilization of seeds and latex, and application of wood and leaves—positions it as a commercially important crop [6, 28, 47]. Among the prominent cultivars in Malaysia, cv. ‘Tekam Yellow’ is favored for its sweetness and pulp quality. However, the industry has recently been threatened by a physiological disorder known as "jackfruit-bronzing," primarily affecting this cultivar.

However, the industry has recently been threatened by *Pantoea stewartii* subsp. *stewartii*, the causal agent of jackfruit bronzing. The infection induces internal discoloration ranging from yellow-orange to reddish hues in the pulp and rag, while the rind remains asymptomatic [3, 20, 26, 30, 54]. This asymptomatic external appearance complicates quality assurance during postharvest handling and marketing, often leading to rejection of produce and significant economic loss.

Detecting internal defects such as bronzing without damaging the fruit is vital to minimize postharvest losses and maintain consumer trust. Non-destructive optical techniques, particularly visible near infrared spectroscopy (Vis-NIRS), have shown promise in the assessment of internal quality attributes in horticultural crops [17, 32]. Vis-NIRS enables rapid, chemical-free measurements by correlating spectral features with physical and chemical properties—primarily via overtone and combination vibrations of C–H, N–H, and O–H molecular bonds [11, 31, 32].

Advanced multivariate modeling techniques such as principal component regression (PCR), partial least squares regression (PLSR), support vector machines (SVM), and artificial neural networks (ANNs) are commonly employed to build predictive models from complex spectral datasets [53].

Among these, PLSR is particularly suitable for highly collinear spectral variables, offering a balance between model interpretability and predictive performance [16].

Previous studies have successfully applied Vis-NIRS in determining internal quality traits—such as firmness, moisture, and sugar content—in fruits including kiwifruit, apples, and citrus [12, 19, 32, 40]. Nevertheless, few studies have explored its application in jackfruit, especially concerning the early detection of internal bronzing. Given the disease's internal nature and economic implications, there is an urgent need for reliable, non-destructive methods to evaluate fruit health.

This study aims to assess the effectiveness of Vis–NIRS in predicting internal bronzing symptoms in cv. 'Tekam Yellow' jackfruit by evaluating firmness and moisture content through the rind at different maturity stages. To achieve this, spectral data were collected from healthy and bronzing-affected fruit at 10, 12, and 14 weeks after anthesis (WAA). Partial least squares regression (PLSR) models were then developed and validated using the spectral dataset. The non-destructive predictions were subsequently compared with destructive reference measurements to determine the accuracy and reliability of the proposed approach.

2 Materials and methods

2.1 Fruit materials

Jackfruit (*Artocarpus heterophyllus* Lam.) cv. 'Tekam Yellow' was obtained from a commercial orchard operated by Agro BS Sdn. Bhd. in Jasin, Melaka, Malaysia. A total of 54 jackfruit syncarps were harvested during the same cropping season, representing three distinct maturity stages: 10, 12, and 14 weeks after anthesis (WAA). Fruit maturity stages at 10, 12, and 14 WAA were selected according to standardized commercial harvesting practices commonly applied for cv. 'Tekam

Yellow' jackfruit production in Malaysia. Nevertheless, future studies should incorporate physicochemical maturity indices such as soluble solids concentration [31], peel color [30], and starch conversion to further strengthen maturity classification.

At each stage, six healthy and six bronzing-affected fruits were collected. Bronzing-affected fruit were identified based on the presence of internal yellowish-orange to reddish discoloration symptoms in the pulp and rag tissues following destructive examination after spectral acquisition, whereas healthy fruit showed no visible internal bronzing symptoms.

Immediately post-harvest, all samples were carefully packaged and transported in ventilated containers under ambient conditions to Universiti Putra Malaysia and analyzed within two hours to minimize physiological deterioration and moisture loss.

2.2 Spectral acquisition

Spectral measurements were conducted on both rind and flesh tissues using a high-resolution visible near-infrared spectrometer (HR4000, Ocean Optics Inc., Dunedin, FL, USA) at the Laboratory of System Technology, Plantation & Mechanization, Institute of Plantation Studies, Universiti Putra Malaysia. Spectra were acquired in reflectance mode across the 200–1100 nm range, with a spectral resolution of 0.5 nm. Although spectral acquisition was conducted within the 200–1100 nm range, only the 500–950 nm region was retained for subsequent analyses because the spectral extremes exhibited low signal-to-noise ratio and increased detector noise.

Each fruit was sectioned into 30 points to obtain localized spectral data (Figure 1). The scanning distance was fixed at 1.5 cm between the probe and sample (Figure 2). Spectral acquisition was performed under controlled laboratory conditions at approximately 25 ± 2 °C. For each sampling

point, spectra were averaged from three consecutive scans to improve spectral stability and minimize instrumental noise.

Illumination was provided by a halogen light source (HL-2000, 12VDC, 15W), which was periodically alternated every 30 minutes to minimize thermal drift and maintain stable illumination intensity throughout prolonged spectral acquisition [40]. A white ceramic reference tile with approximately 100% reflectance was used to calibrate the instrument before each measurement session. The reference surface was kept free of dust and contaminants to ensure accurate calibration [1, 2, 31].

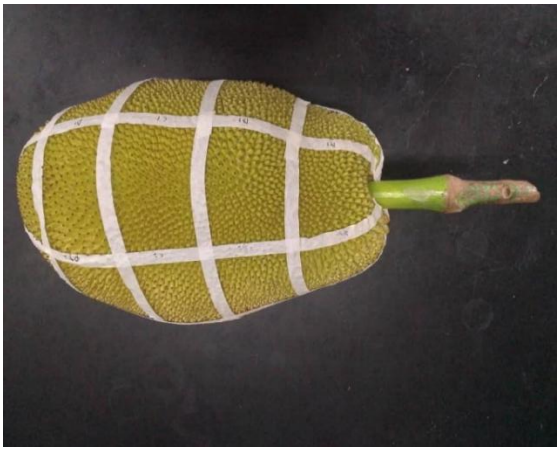

Fig. 1 Divided 30 portions from top to bottom

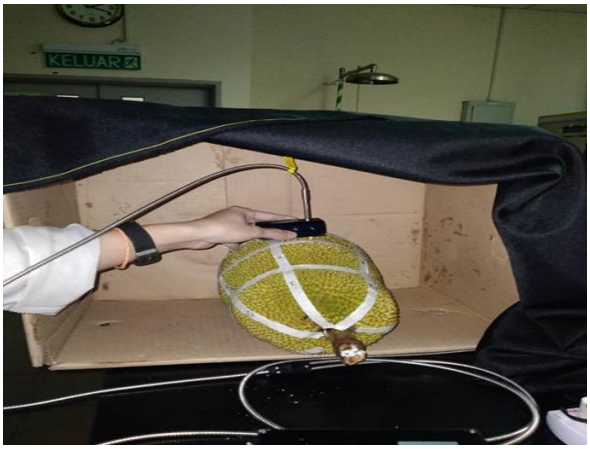

Fig. 2 Radiation penetrated on the rind on each portion using spectrometer

2.3 Reference methods

2.3.1 Firmness of flesh and rind

Mechanical firmness of rind and flesh (seed removed) was measured using an Instron 5545 texture analyzer equipped with a 6 mm cylindrical probe. Penetration was performed at 25 mm min^{-1} to a depth of 10 mm within the equatorial region of the fruit. For each tissue type, three destructive

measurements were taken in tissue regions corresponding to the spectral acquisition zones to maintain spatial consistency between spectral and reference data; the three readings were averaged and expressed in Newtons (N) [36]. The system was controlled using Merlin software (Version M12-13664-EN).

2.3.2 Moisture content of rind, flesh, and seed

Moisture and dry matter of rind, flesh, and seed were determined gravimetrically [14, 36]. An initial mass (A) of an empty moisture envelope was recorded using a calibrated digital balance (Model EIC-600H, A&D Company, Japan). Subsequently, 5 g of each sample component was weighed into the envelope (mass B). Moisture measurements for each tissue type were conducted in triplicate to minimize analytical variability. Samples were dried in a convection oven maintained at 78 ± 2 °C for four days until constant weight was achieved; repeated weighing was performed to confirm constant dry weight. The final dry mass (D) was recorded post-drying. Wet weight of fresh sample and weight of dry sample were calculated as:

Wet weight of fresh sample, $C = B - A$

Weight of dry sample, $E = D - A$

Moisture content (%, wet basis) and dry matter content (%) were calculated as:

Moisture content (%) = $[(C - E) / C] \times 100\ \%$

Dry matter content (%) = 100 % – (% w.b.)

All values reported are the averages of three replicates.

2.4 Multivariate and statistical analyses

Descriptive statistics were first computed to characterize the dataset. Spectral data were processed and analyzed using The Unscrambler X 10.3 software (CAMO Software AS, Oslo, Norway). Partial least squares regression (PLSR) was used as the primary calibration model, while Multiple Linear Regression (MLR), Principal Component Regression (PCR), and Support Vector Regression (SVR) were additionally evaluated for comparative purposes.

A total of 54 fruits were analyzed, generating 1,620 spectra obtained from 30 sampling points per fruit. For each maturity stage, datasets were partitioned into calibration (75%) and validation (25%) subsets. To avoid potential data leakage and spectral dependency, dataset partitioning was performed at the fruit level rather than at the individual spectrum level. All spectra originating from a single fruit were assigned exclusively to either the calibration dataset or the validation dataset. The calibration set comprised 1,215 spectra, while the validation set included 405 spectra.

Different spectral preprocessing methods, including moving average, Gaussian filter, median filter, Savitzky–Golay smoothing, standard normal variate (SNV), baseline correction, and multiplicative scatter correction (MSC), were evaluated prior to model development. Model optimization involved comparison among PLSR, PCR, MLR, and SVR algorithms using different spectral preprocessing combinations and latent variable (LV) settings to identify the best-performing predictive models.

For PLSR and PCR models, the optimal number of latent variables was selected based on minimization of cross-validation prediction error while avoiding model overfitting [5] Future

160 studies should incorporate external validation using independent harvest seasons and orchards to
161 further evaluate model robustness and generalizability.

162 Model performance was evaluated using the coefficient of determination (R^2), root mean square
163 error of calibration (RMSEC), root mean square error of prediction (RMSEP), bias, and residual
164 predictive deviation (RPD). The equations used were as follows:

165 The accuracy of the PLS models was denoted by the R^2 (Eq. 1), $RMSE_C$ (Eq. 2) and $RMSE_v$ (Eq.
166 3) that act as an indicator of the best fitting of the predicted values [31].

167 $$R^2 = 1 - \frac{\sum_{i=1}^{n}(\hat{y}i - yi)^2}{\sum_{i=1}^{n}(\hat{y}i - ym)^2} \qquad \text{(Eq. 1)}$$

168 $$RMSEC = \sqrt{\frac{1}{nc-1}\sum_{i=1}^{nc}(\hat{y}i - yi)^2} \qquad \text{(Eq. 2)}$$

169 $$RMSEV = \sqrt{\frac{1}{nv-1}\sum_{i=1}^{nv}(\hat{y}i - yi - bias)^2} \qquad \text{(Eq. 3)}$$

170 Which n is the number of the data sample, n_c is the of data sample for calibration, n_v is the number
171 of data sample for validation, $\hat{y}_i$ is the prediction value, y_i is measured value and y_m is mean value.
172 The average differences between predicted and actual values were considered as bias (Eq. 4), while
173 residual predictive deviation value (RPD) was calculated according to Eq. 5 [31].

174 Residual predictive deviation (RPD) was calculated as the ratio between the standard deviation
175 (SD) of the reference validation dataset and the root mean square error of prediction (RMSEP).
176 All RPD values reported in the revised manuscript were recalculated according to standard
177 chemometric procedures.

$$Bias = \frac{1}{\mathrm{nv}}\sum_{i=1}^{nv}(\hat{y}\mathrm{i} - \mathrm{yi}) \qquad \text{(Eq. 4)}$$

$$RPD = \frac{\mathrm{SD}}{\mathrm{RMSEP}} \qquad \text{(Eq. 5)}$$

The analytical workflow diagram was revised to accurately represent fruit sampling, spectral acquisition, preprocessing procedures, calibration model development, validation processes, and statistical analyses conducted in the present study, as illustrated in Figure 3.

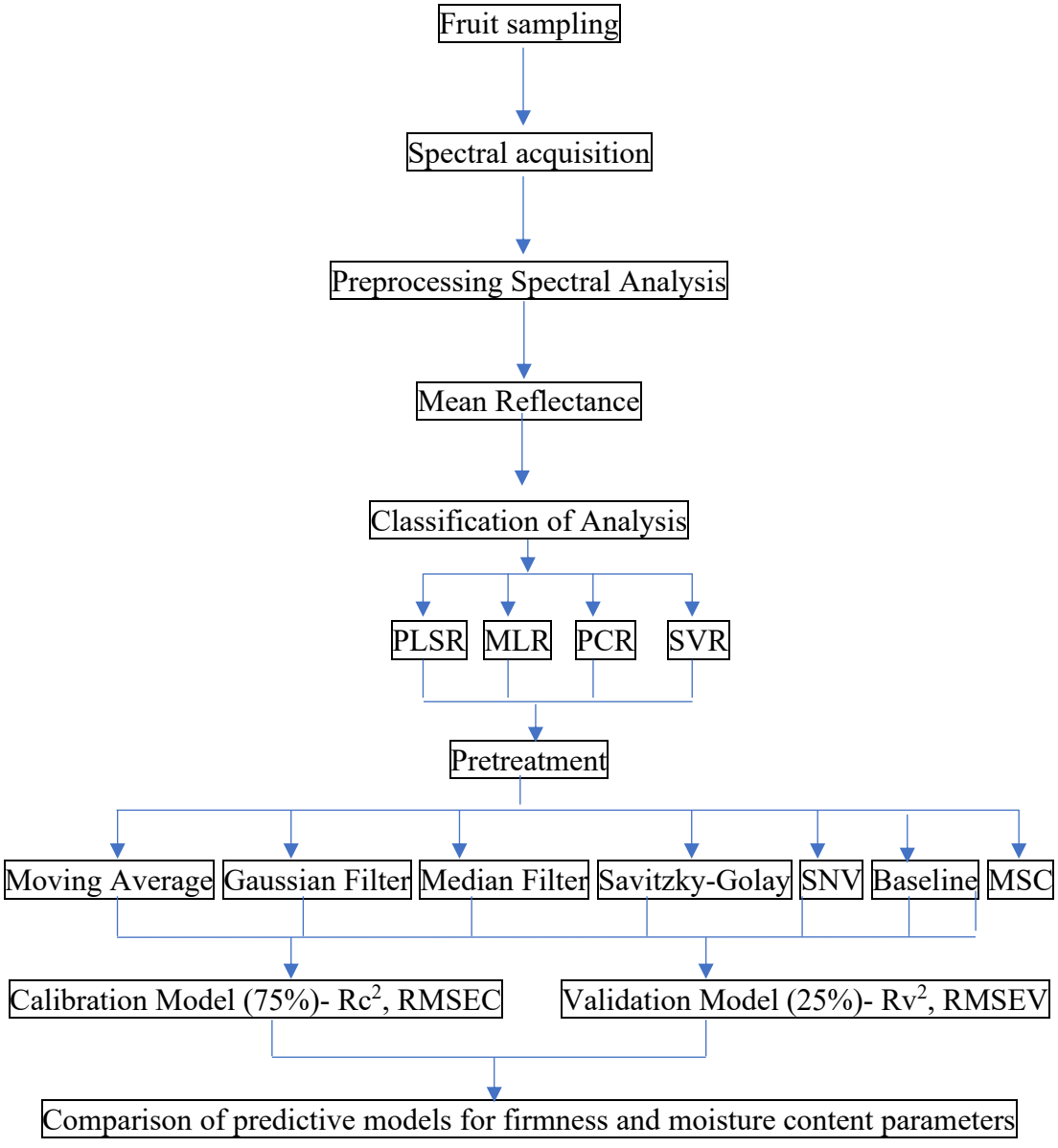

Fig. 3 Flowchart of spectral preprocessing and data analysis for predicting jackfruit fruit quality.

All statistical analyses, including analysis of variance (ANOVA), were performed using R software (version 4.0.4; R Core Team, 2021). Significant differences in firmness and moisture content between bronzing and non-bronzing jackfruit samples at different maturity stages were determined using Fisher's protected least significant difference (LSD) test at $p \leq 0.05$.

3. Result

3.1 Physicochemical characteristics of healthy and bronzing jackfruit

3.1.1 Firmness dynamics across fruit tissues

The firmness of the jackfruit rind was not significantly influenced by the interaction between weeks after anthesis (WAA) and fruit health status (H), as shown in Table 1. In contrast, a significant WAA × H interaction effect was observed on the firmness of the flesh tissue (Table 1). No statistically significant differences in rind firmness were detected between normal and bronzing-affected fruit of jackfruit cv. 'Tekam Yellow'. However, flesh firmness showed a marked reduction in bronzing-affected fruit compared to normal counterparts (Table 1). The significant interaction between maturity stage and fruit health status suggested that bronzing disorder influenced tissue firmness differently across developmental stages.

In general, unripe fruit exhibited greater firmness in both rind and flesh tissues compared to fruit at more advanced maturity stages. A consistent and significant decline in flesh firmness was observed with increasing maturity (Figure 4). The reduction in tissue firmness observed with increasing maturity may be associated with cell wall degradation, pectin solubilization, and

progressive softening processes during fruit ripening. The WAA × H interaction further revealed that flesh firmness varied notably with fruit health status, particularly at 10 WAA and 14 WAA. However, no significant differences in flesh firmness between normal and bronzing-affected fruit were recorded at 12 WAA (Figure 4).

Peak rind firmness was recorded at 61.49 N in bronzing-affected fruit at 12 WAA, whereas the lowest value was observed at 33.09 N in normal fruit at 14 WAA (Table 2). For the flesh, the highest firmness was 355.45 N in bronzing-affected fruit at 10 WAA, while the lowest was 43.24 N in normal fruit at 14 WAA (Figure 4; Table 3). The observed variability among samples was likely associated with heterogeneous bronzing severity, biological differences among fruit tissues, and maturity-dependent physiological changes.

Table 1 Main and interaction effects of weeks after anthesis and fruit health status on the rind and flesh firmness of jackfruit cv. 'Tekam Yellow'.

Factor	Rind Firmness (N)	Flesh Firmness(N)
Weeks after anthesis (WAA)		
W10	47.02b[x]	334.01a
W12	56.16a	299.75b
W14	36.97c	136.74c
Fruit health status (H)		
Normal (N)	42.53a	217.69b
Bronzing (B)	50.71a	293.16a
Interaction		
WAA x H	NS	***

[x]Means followed by different letters within each factor were significantly different according to Fisher's protected LSD test at $p \leq 0.05$. NS and *** indicate non-significant and highly significant differences at $p \leq 0.001$, respectively.

Table 2 Mean ± standard deviation of rind firmness for healthy and bronzing-affected fruit at different maturity stages (weeks after anthesis).

Healthiness	WAA	Mean	SD	Interaction of Healthiness within Weeks	Pretreatment
Healthy	10	43.80cd	18.00	***	SG + SNV

Bronzing	10	49.60bc	20.35	***	SG + SNV
Healthy	12	50.83b	24.84	***	SG + SNV
Bronzing	12	61.49a	22.01	***	SG + SNV
Healthy	14	33.09e	25.49	**	SG + SNV
Bronzing	14	40.84d	32.04	**	SG + SNV

Means followed by different letters were significantly different according to Fisher's protected LSD test at $p \leq 0.05$.

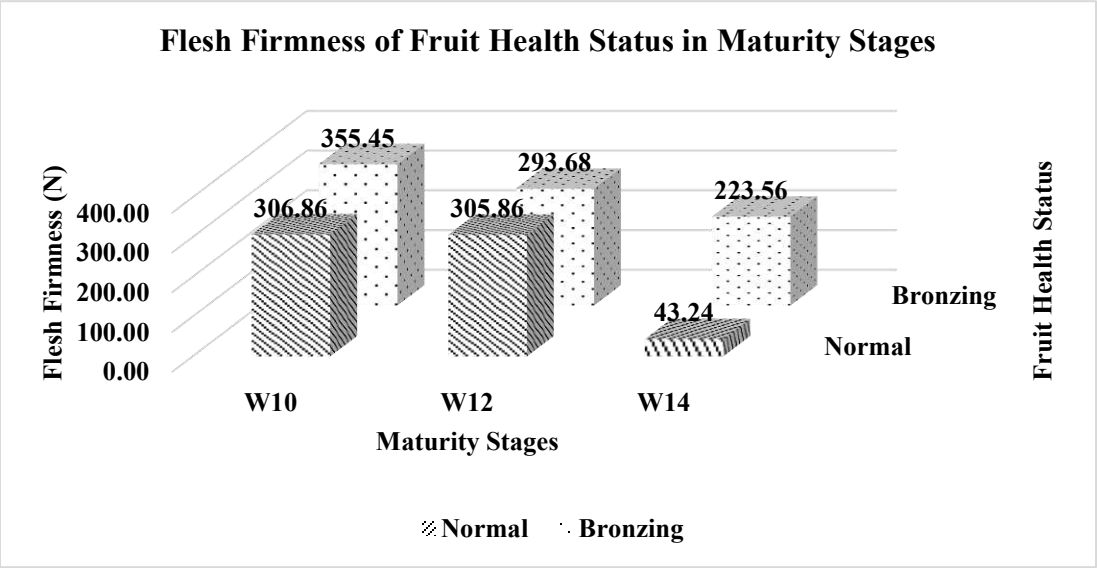

Fig. 4 Effects of fruit health status and maturity stage (weeks after anthesis) on the flesh firmness of jackfruit cv. 'Tekam Yellow'. Means followed by different uppercase and lowercase letters are significantly different at $p \leq 0.05$ according to Fisher's protected LSD for fruit health status and maturity stage, respectively.

Table 3 Mean ± standard deviation of flesh firmness for healthy and bronzing-affected fruit at different maturity stages (weeks after anthesis).

Healthiness	WAA	Mean	SD	Interaction of Healthiness within Weeks	Pretreatment
Healthy	10	306.863b	124.30	***	SNV + MSC
Bronzing	10	355.453a	188.54	***	SG + SNV
Healthy	12	305.862b	246.31	NS	NS
Bronzing	12	293.683b	143.54	NS	NS

Healthy	14	43.243d	19.35	***	SG + SNV
Bronzing	14	223.562c	135.04	***	SNV + MSC

Means followed by different letters were significantly different according to Fisher's protected LSD test at $p \leq 0.05$.

The result tables were reorganized to improve clarity and to separate spectral preprocessing information from physicochemical measurements.

3.1.2 Moisture content dynamics across fruit tissues

The analysis revealed no statistically significant interaction between weeks after anthesis (WAA) and fruit health status (H) on the rind moisture content of jackfruit cv. 'Tekam Yellow' (Table 4). However, significant WAA × H interactions were observed for moisture content in the flesh and seed tissues. Comparing fruit health conditions, significant differences were evident in moisture content across all three tissues—rind, flesh, and seed—between normal and bronzing-affected fruit. Specifically, bronzing-affected fruit exhibited elevated moisture levels in both the flesh and seeds, whereas a reduction in rind moisture content was recorded relative to normal fruit. Increased moisture content in bronzing-affected tissues may be associated with physiological disruption of cellular structure and altered water distribution during disease progression. Similar moisture accumulation patterns associated with tissue deterioration and physiological disorders have also been reported in several climacteric fruit systems [25, 29, 42].

Fruit maturity exerted a significant influence on flesh and seed moisture dynamics (Table 4). The significant WAA × H interaction confirmed that moisture content in the flesh and seeds increased substantially with maturity, particularly from 10 WAA to 14 WAA. However, for flesh moisture content, no significant difference was detected at 10 WAA between normal and bronzing-affected fruit (Figure 5 and Table 6). The combined effects of fruit maturity and bronzing status were

considered in the statistical analysis to minimize potential confounding influences on firmness and moisture predictions.

Peak rind moisture content was recorded at 85.02% (wet basis) in normal fruit at 10 WAA, whereas the lowest value was observed at 82.44% in bronzing-affected fruit at 14 WAA (Table 5). For the flesh, the highest moisture content was 73.53% in bronzing-affected fruit at 14 WAA, while the lowest was 69.17% in normal fruit at 10 WAA (Figure 5; Table 6). Similarly, seed moisture content peaked at 68.66% in bronzing-affected fruit at 14 WAA and was lowest at 58.42% in normal fruit at 12 WAA (Figure 6; Table 7). Although statistically significant differences were observed, the practical relevance of these changes should also be considered in relation to industrial grading and postharvest quality management applications.

Table 4 Main and interaction effects of weeks after anthesis and fruit health status on the rind, flesh, and seed moisture content of jackfruit cv. 'Tekam Yellow'.

Factor	Rind Moisture Content (% w.b.)	Flesh Moisture Content (% w.b.)	Seed Moiture Content (% w.b.)
Weeks after anthesis (WAA)			
W10	84.66a[x]	69.19b	62.07b
W12	84.44a	69.71b	62.32b
W14	82.79b	72.62a	65.61a
Fruit health status (H)			
Normal (N)	84.18a	69.52b	60.22b
Bronzing (B)	83.76b	71.38a	66.04a
Interaction			
WAA x H	NS	***	***

[x]Means followed by different letters within each factor were significantly different according to Fisher's protected LSD test at $p \leq 0.05$. NS and *** indicate non-significant and highly significant differences at $p \leq 0.001$, respectively.

Table 5 Mean ± standard deviation of rind moisture content for healthy and bronzing-affected fruit at different maturity stages (weeks after anthesis).

Healthiness	WAA	Mean	SD	Interaction of Healthiness within WAA	Pretreatment

Healthy	10	85.02a	1.39	***	SNV + MSC
Bronzing	10	84.38a	2.08	***	SG + SNV
Healthy	12	84.48a	2.45	NS	NS
Bronzing	12	84.39a	2.33	NS	NS
Healthy	14	83.15b	3.14	*	SNV + MSC
Bronzing	14	82.44c	4.37	*	SG + SNV

Means followed by different letters were significantly different according to Fisher's protected LSD test at $p \leq 0.05$

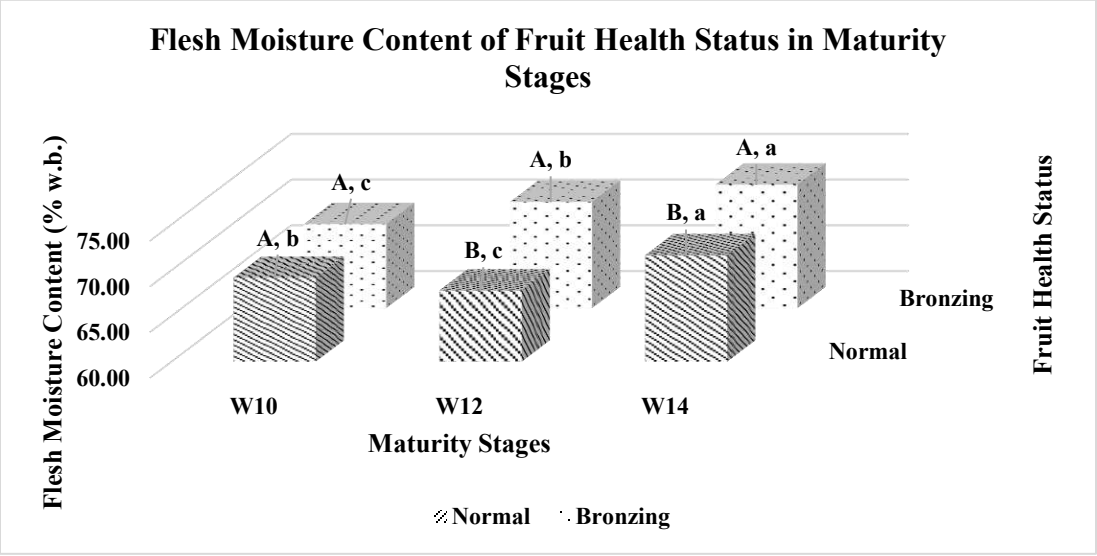

Fig. 5 Effects of fruit health status and maturity stage (weeks after anthesis) on the flesh moisture content of jackfruit cv. 'Tekam Yellow'. Means followed by different uppercase and lowercase letters are significantly different at $p \leq 0.05$ according to Fisher's protected LSD for fruit health status and maturity stage, respectively.

Table 6 Mean ± standard deviation of flesh moisture content for healthy and bronzing-affected at different maturity stages (weeks after anthesis).

Healthiness	WAA	Mean	SD	Interaction of Healthiness within WAA	Pretreatment
Healthy	10	69.17c	0.23	NS	NS
Bronzing	10	69.21c	0.31	NS	NS
Healthy	12	67.785d	3.29	***	SG + SNV

Bronzing	12	71.641b	4.48	***	SG + SNV
Healthy	14	71.636b	4.92	***	SG + SNV
Bronzing	14	73.526a	7.49	***	SG + SNV

Means followed by different letters were significantly different according to Fisher's protected LSD test at $p \leq 0.05$

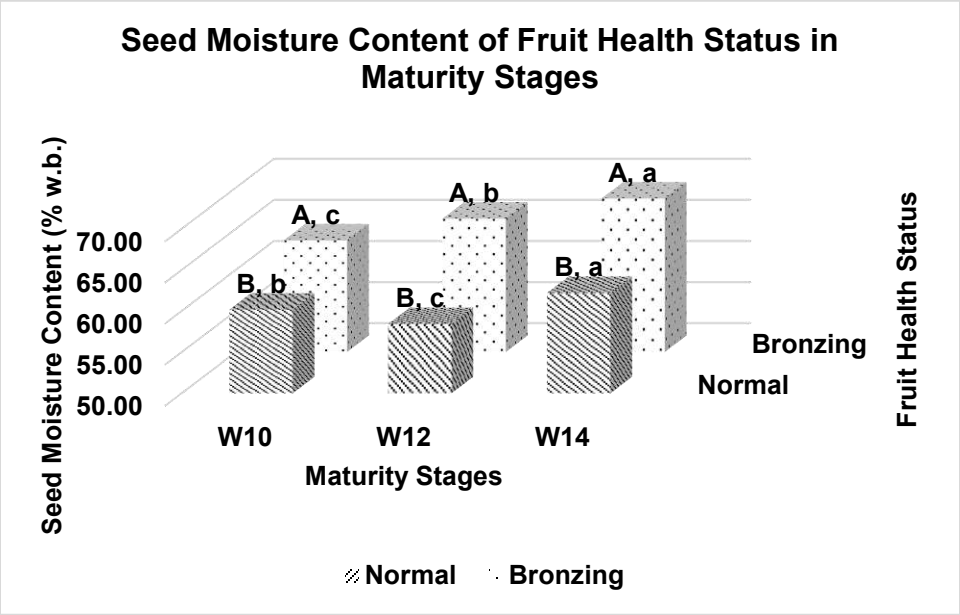

Fig. 6 Effects of fruit health status and maturity stage (weeks after anthesis) on the seed moisture content of jackfruit cv. 'Tekam Yellow'. Means followed by different uppercase and lowercase letters are significantly different at $p \leq 0.05$ according to Fisher's protected LSD for fruit health status and maturity stage, respectively.

Table 7 Mean ± standard deviation of seed moisture content for healthy and bronzing-affected jackfruit at different maturity stages (weeks after anthesis).

Healthiness	WAA	Mean	SD	Interaction of Healthiness within WAA	Pretreatment
Healthy	10	60.16d	5.65	***	SG + MSC
Bronzing	10	63.58c	6.56	***	SG + SNV
Healthy	12	58.42e	7.24	***	SG + SNV
Bronzing	12	66.22b	7.54	***	SG + SNV
Healthy	14	62.19c	11.04	***	SG + SNV
Bronzing	14	68.66a	7.54	***	SG + SNV

Means followed by different letters were significantly different according to Fisher's protected LSD test at $p \leq 0.05$

The result tables were reorganized to improve clarity and to separate spectral preprocessing information from physicochemical measurements.

3.2 Spectral characteristics of jackfruit rind

Figures 7 and 8 illustrate the raw spectral reflectance profiles of healthy and bronzing-affected jackfruit fruit at 10 weeks after anthesis (WAA). In contrast, Figures 9 and 10 present the corresponding preprocessed Vis–NIR spectra derived from a total of 1,620 samples. As previously reported in the literature, most absorption features within the Vis–NIR region originate from overtones and combination bands of fundamental molecular vibrations in the mid-infrared region, resulting in broad and overlapping spectral features characteristic of complex biological matrices such as fruits and vegetables [31, 40].

The unprocessed spectral data obtained from healthy jackfruit at 10 WAA exhibited typical scattering effects and baseline shifts associated with heterogeneous rind surface properties and internal tissue variability (Figure 7). Similar spectral distortions were observed in bronzing-affected jackfruit rind at 10 WAA (Figure 8), indicating that physiological disorders may alter light absorption and scattering behavior within the fruit tissues. Subsequent preprocessing using Savitzky–Golay smoothing and Standard Normal Variate (SNV) transformation (Figures 9 and 10) substantially improved spectral consistency by reducing baseline variation, minimizing scattering interference, and enhancing the visibility of subtle absorption features relevant for chemometric modeling.

The pretreated spectra revealed pronounced absorption patterns within the visible to near-infrared region, particularly between 500 and 950 nm (Figures 9 and 10). Distinct absorption bands were

observed at approximately 760 nm and 970 nm, consistent with spectral characteristics previously reported for durian pulp [45]. These absorption features were primarily associated with O–H overtone absorption related to tissue water content within the analyzed spectral range [41]. Nevertheless, spectral interpretation within biological tissues should be approached cautiously because overlapping absorption bands may simultaneously reflect combined contributions from water molecules, tissue structure, light scattering effects, and other biochemical constituents.

To further investigate spectral heterogeneity within the fruit, each jackfruit rind was divided into thirty sampling regions distributed across five latitudinal layers: top (A1–A6), middle-top (B1–B6), middle (C1–C6), middle-bottom (D1–D6), and bottom (E1–E6). The average spectral reflectance profiles obtained from these regions demonstrated noticeable spatial variability, indicating non-uniform physiological and biochemical distribution across the rind tissues. Such spatial variability may contribute to the predictive capability of the developed calibration models by capturing localized physiological responses associated with bronzing development and fruit maturation.

Both healthy and bronzing-affected fruit displayed characteristic absorption peaks centered around 675 nm and 945 nm (Figures 9 and 10). A strong absorption feature near 970 nm was consistently detected and likely corresponded to the second overtone of water, as similarly observed in apple fruit tissues [39]. Broad absorption features within the 940–970 nm region were mainly associated with overlapping water-related and structural spectral responses, which have also been reported in passion fruit studies [35]. Although these spectral regions may exhibit indirect associations with sugar-related compounds such as sucrose and fructose, interpretation should remain cautious because direct quantification of individual sugars was not performed in the present study. Similar

limitations regarding selective biochemical interpretation of Vis–NIR spectra in complex biological materials have been highlighted in previous fruit quality assessment studies [23].

Collectively, these findings demonstrate the capability of Vis–NIR spectroscopy to capture physiologically meaningful spectral information associated with tissue water dynamics, structural heterogeneity, and maturity-related biochemical variation in jackfruit rind. The observed spectral characteristics provide valuable insights into fruit physiological status and further support the potential application of Vis–NIR spectroscopy as a rapid and non-destructive tool for postharvest quality evaluation and bronzing detection in jackfruit.

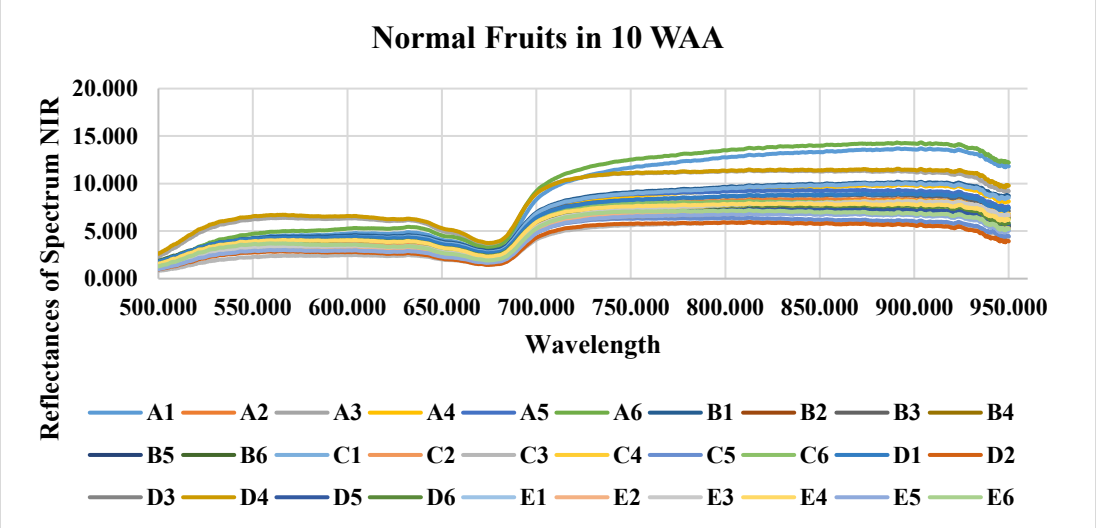

*The rind was systematically segmented into five layers—top (A1 to A6), middle-top (B1 to B6), middle (C1 to C6), middle-bottom (D1 to D6), and bottom (E1 to E6)—to assess spatial spectral variability.

Fig. 7 Mean spectral reflectance of 30 portions of raw material from normal fruit at 10.

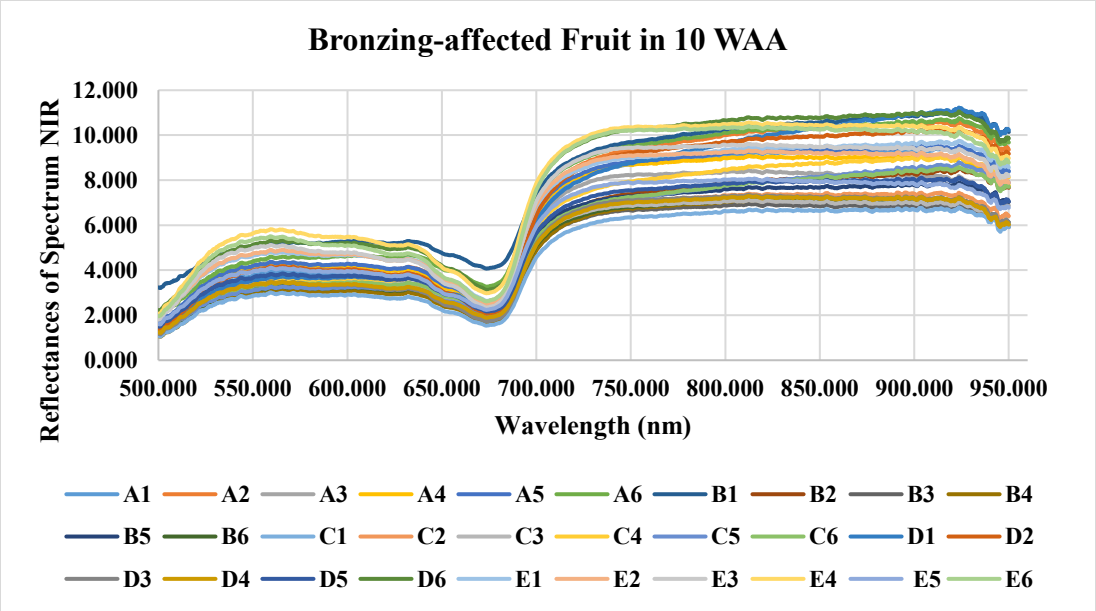

*The rind was systematically segmented into five layers—top (A1 to A6), middle-top (B1 to B6), middle (C1 to C6), middle-bottom (D1 to D6), and bottom (E1 to E6)—to assess spatial spectral variability.

Fig. 8 Mean spectral reflectance of 30 portions of raw material from bronzing-affected fruit at 10 WAA.

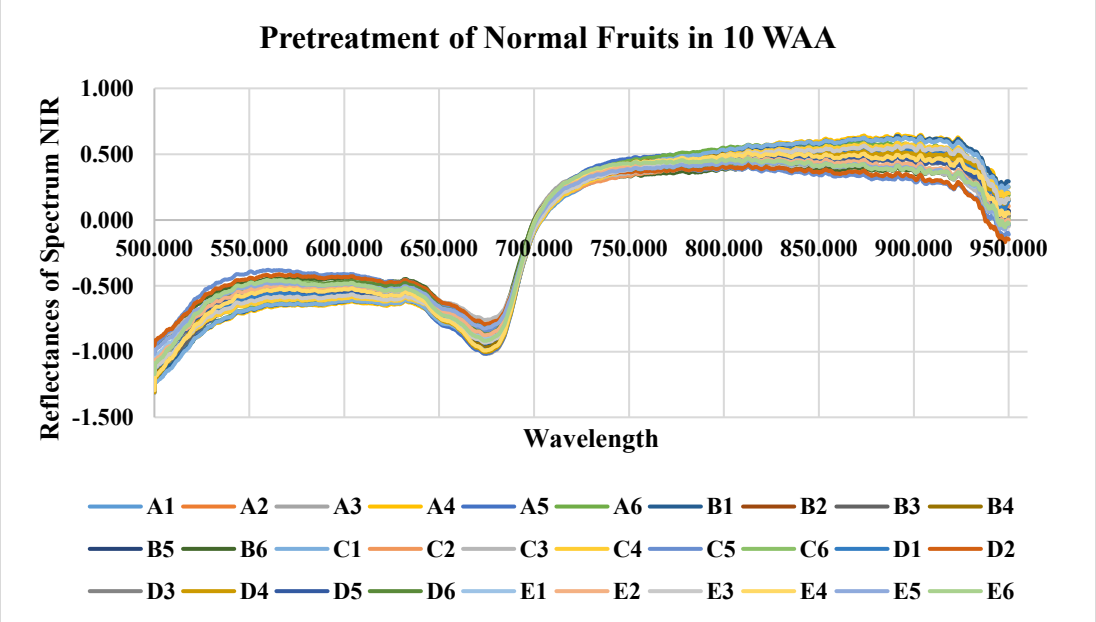

*The rind was systematically segmented into five layers—top (A1 to A6), middle-top (B1 to B6), middle (C1 to C6), middle-bottom (D1 to D6), and bottom (E1 to E6)—to assess spatial spectral variability.

Fig. 9 Pre-treated mean Vis–NIR reflectance spectrum of normal fruit (30 portions) at 10 WAA, preprocessed using Savitzky–Golay smoothing and SNV.

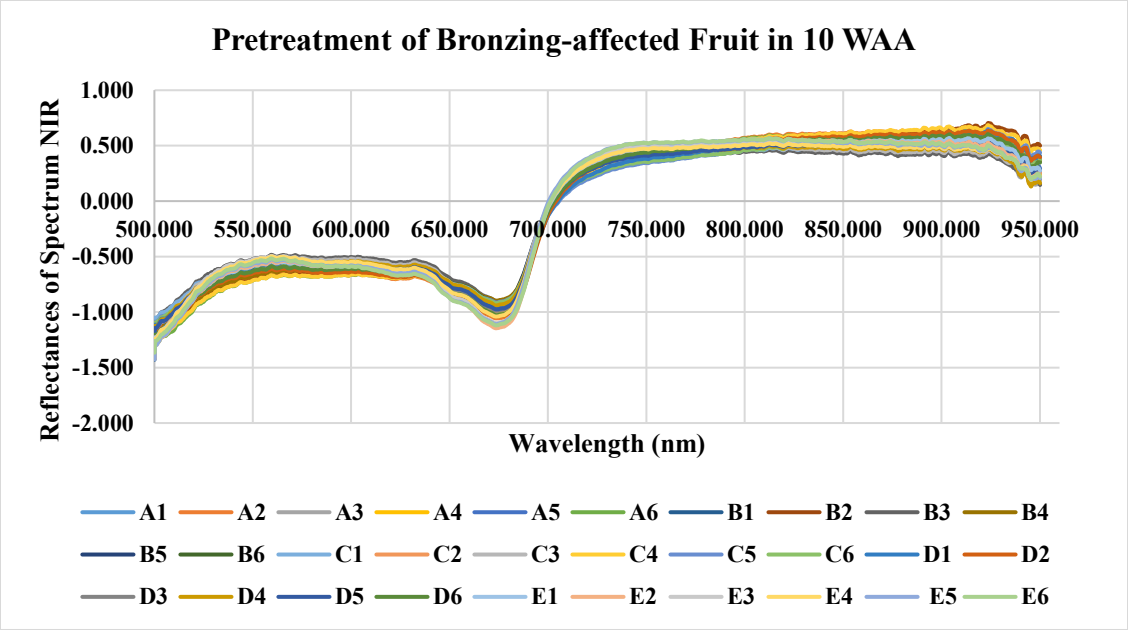

*The rind was systematically segmented into five layers—top (A1 to A6), middle-top (B1 to B6), middle (C1 to C6), middle-bottom (D1 to D6), and bottom (E1 to E6)—to assess spatial spectral variability.

Fig. 10 Pre-treated mean Vis–NIR reflectance spectrum of bronzing-affected fruit (30 portions) at 10 WAA, preprocessed using Savitzky–Golay smoothing and SNV.

3.3 Predictive performance of PLSR models using twelve spectral preprocessing methods

3.3.1 Predictive performance of PLSR models for jackfruit rind firmness at 10 WAA, 12 WAA and 14 WAA

The predictive performance of Vis–NIR partial least squares regression (PLSR) models for jackfruit rind firmness was evaluated at 10, 12, and 14 weeks after anthesis (WAA) across the 500–950 nm spectral range for both healthy and bronzing-affected fruit. All evaluated preprocessing combinations and calibration model performances were reported to provide transparent comparison of predictive outcomes and to minimize potential bias associated with selective reporting of only the best-performing models.

Overall, Savitzky–Golay (SG) smoothing alone or combined with Standard Normal Variate (SNV) consistently produced superior predictive performance compared with other preprocessing approaches. The improvement observed after SG and SNV preprocessing indicated that reducing

baseline variation and scattering interference enhanced the extraction of relevant spectral information associated with rind firmness, consistent with previous Vis–NIR spectroscopy studies involving fruit quality assessment and firmness prediction in climacteric fruits [4, 10].

At 10 WAA, the SG+SNV-preprocessed model with six latent variables (LVs) for healthy rind achieved strong calibration and validation performance with $Rc^2 = 0.95$, RMSEc = 0.94, $Rv^2 = 0.95$, and RMSEv = 0.93 (Table 8). Similarly, bronzing-affected rind with seven LVs produced $Rc^2 = 0.93$, RMSEc = 1.06, $Rv^2 = 0.94$, and RMSEv = 1.03. The close agreement between calibration and validation statistics indicated stable predictive performance with minimal evidence of substantial overfitting. Comparable improvements following SG-based preprocessing have also been reported for firmness prediction in kiwifruit using Vis–NIR spectroscopy [4, 10]. Figures 11 and 12 present the measured versus predicted rind firmness for healthy and bronzing-affected fruit, respectively.

At 12 WAA, SG+SNV preprocessing further improved predictive performance. Healthy fruit models with three LVs achieved $Rc^2 = 0.96$, RMSEc = 1.29, $Rv^2 = 0.94$, and RMSEv = 1.50, while bronzing-affected rind models with five LVs yielded $Rc^2 = 0.95$, RMSEc = 1.18, $Rv^2 = 0.95$, and RMSEv = 1.23 (Table 9). Residual plots and error distribution analyses were additionally evaluated to assess model stability and identify potential systematic prediction bias. The relatively small differences between calibration and validation errors suggested acceptable model generalization within the evaluated dataset, consistent with previous Vis–NIR studies on climacteric fruit quality prediction [10, 21]. However, the exceptionally high R^2 values obtained for several preprocessing combinations should be interpreted cautiously because model performance may still be influenced by sample homogeneity, relatively limited dataset size, and

similarity between calibration and validation subsets. Figures 13 and 14 illustrate the measured versus predicted rind firmness at 12 WAA.

At 14 WAA, healthy rind models showed slightly lower predictive performance, with SG+SNV preprocessing and seven LVs producing $Rc^2 = 0.88$, RMSEc = 1.49, $Rv^2 = 0.88$, and RMSEv = 1.43 (Table 10). The reduced prediction accuracy at advanced maturity stages may reflect lower firmness variability and increased tissue softening as fruit approached full ripeness. In contrast, bronzing-affected rind maintained relatively high predictive performance with four LVs ($Rc^2 = 0.91$, RMSEc = 1.56, $Rv^2 = 0.91$, and RMSEv = 1.50), suggesting that disorder-associated physiological changes contributed additional spectral information relevant for firmness prediction. Similar observations regarding the influence of physiological variability and tissue heterogeneity on predictive performance have been reported in studies involving texture characterization and internal disorder detection in climacteric fruit systems [4, 7, 21]. Figures 15 and 16 depict the measured versus predicted rind firmness for healthy and bronzing-affected fruit at 14 WAA.

Model performance varied across maturity stages, indicating that tissue development, ripening progression, and bronzing severity influenced spectral predictability during fruit maturation. Earlier maturity stages generally demonstrated stronger predictive performance, whereas advanced maturity stages exhibited slightly greater prediction variability due to increased physiological heterogeneity and tissue softening effects.

Collectively, these findings demonstrate that SG and SG+SNV-preprocessed Vis–NIR spectroscopy combined with optimized latent variable selection can provide a reliable and non-destructive approach for monitoring rind firmness throughout fruit development, in agreement with previous applications of Vis–NIR spectroscopy for fruit quality assessment and postharvest

monitoring [4, 10, 21]. Although the developed models demonstrated strong internal validation performance, additional external validation using independent harvest seasons, orchards, and larger datasets is necessary to confirm long-term robustness and broader applicability under commercial production conditions.

Table 8 Performance of partial least squares regression (PLSR) models for predicting rind firmness of jackfruit cv. 'Tekam Yellow' at 10 weeks after anthesis using different Vis–NIR spectral preprocessing methods for calibration and validation datasets.

			Healthy Fruit					Bronzing-affected Fruit		
P1	**Lvs**	**Rv²**	**RMSEv**	**Rc²**	**RMSEc**	**Lvs**	**Rv²**	**RMSEv**	**Rc²**	**RMSEc**
Raw	6	0.14	16.42	0.17	15.65	6	0.10	18.98	0.11	19.32
MV	7	0.21	5.75	0.23	5.57	7	0.14	7.21	0.16	7.18
GF	6	0.14	13.76	0.17	13.13	6	0.10	15.97	0.10	16.25
MF	7	0.19	1.45	0.19	1.40	7	0.10	5.17	0.11	5.52
SG	7	0.21	5.75	0.23	5.57	7	0.14	7.20	0.16	7.18
SNV	7	0.37	3.44	0.40	3.27	7	0.40	3.72	0.40	3.73
SG*	**6**	**0.95**	**0.93**	**0.95**	**0.94**	**7**	**0.94**	**1.03**	**0.93**	**1.06**
B	6	0.15	16.55	0.18	15.82	7	0.15	18.48	0.17	18.61
SG+B	7	0.23	5.73	0.25	5.57	7	0.15	7.20	0.17	7.16
SNV*	6	0.22	3.69	0.26	3.51	7	0.33	3.79	0.31	3.83
MSC	7	0.37	14.90	0.40	14.17	7	0.47	19.68	0.48	19.64
SG**	2	0.98	2.09	0.98	2.06	2	0.99	2.79	0.99	2.81
SNV**	7	0.36	3.40	0.39	3.23	7	0.42	3.75	0.42	3.75

P1 = Pretreatment 1, Raw = Raw data, MV = Moving Average, GF = Gaussian Filter, MF = Median Filter, SG = Savitzky-Golay, SNV = Standard Normal Variate, SG* = Savitzky-Golay + Standard Normal Variate, B = Baseline, SG+B = Savitzky-Golay + Baseline, SNV* = Standard Normal Variate + Baseline, MSC = Multiplicative Scatter Correction, SG** = Savitzky-Golay + Multiplicative Scatter Correction, SNV** = Standard Normal Variate + Multiplicative Scatter Correction, respectively.

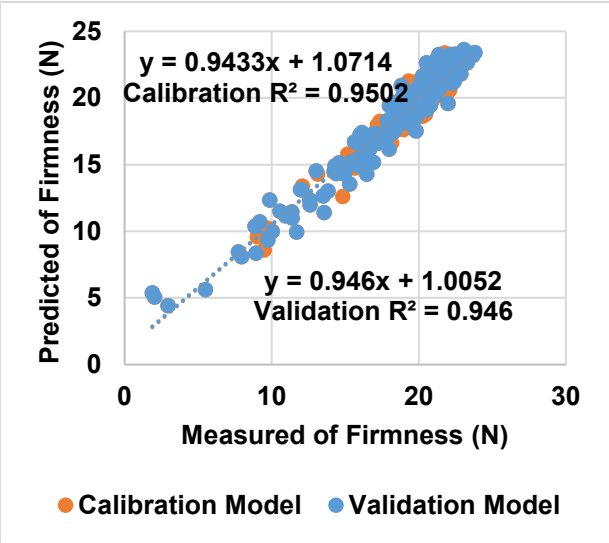

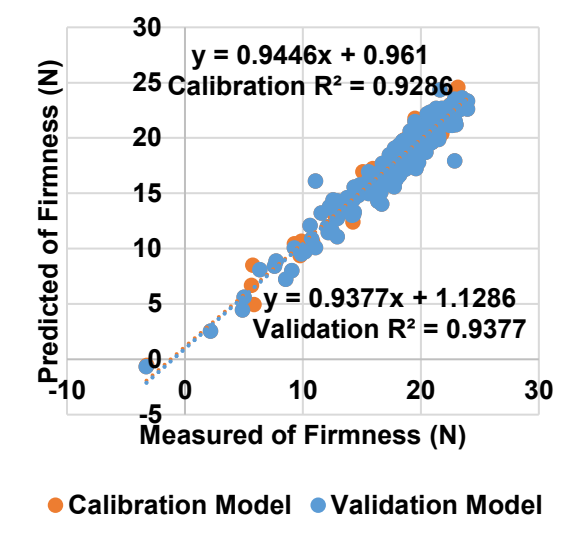

Fig. 11 (Left) Measured versus predicted healthy rind firmness at 10 weeks after anthesis from reflectance spectral data for calibration and validation models.
Fig. 12 (Right) Measured versus predicted bronzing-affected fruit rind firmness at 10 weeks after anthesis from reflectance spectral data for calibration and validation models.

Performance of partial least squares regression (PLSR) models for predicting rind firmness of jackfruit cv. 'Tekam Yellow' at 12 weeks after anthesis using different Vis–NIR spectral preprocessing methods for calibration and validation datasets.

Table 9 Performance of partial least squares models for predicting rind firmness of jackfruit *cv.* 'Tekam Yellow' at 12 weeks after anthesis using different Vis–NIR spectral preprocessing methods for calibration and validation datasets.

			Healthy Fruit					Bronzing-affected Fruit		
P1	**Lvs**	**Rv²**	**RMSEv**	**Rc²**	**RMSEc**	**Lvs**	**Rv²**	**RMSEv**	**Rc²**	**RMSEc**
Raw	7	0.36	19.65	0.31	20.19	7	0.14	20.10	0.15	19.87
MV	7	0.37	19.71	0.31	20.25	7	0.19	6.83	0.19	6.72
GF	7	0.37	17.23	0.32	17.87	7	0.14	16.78	0.14	16.60
MF	7	0.15	4.59	0.11	4.96	6	0.05	4.69	0.01	4.22
SG	6	0.27	16.00	0.20	17.25	7	0.19	6.83	0.19	6.72
SNV	7	0.69	3.41	0.66	3.50	7	0.61	3.60	0.62	3.53
SG*	**3**	**0.94**	**1.50**	**0.96**	**1.29**	**5**	**0.95**	**1.23**	**0.95**	**1.18**
B	7	0.34	19.87	0.29	20.29	7	0.11	20.30	0.12	20.05
SG+B	7	0.27	15.98	0.21	17.23	7	0.23	1.84	0.24	6.75

SNV*	7	0.60	3.73	0.56	3.81	7	0.57	3.54	0.59	3.48
MSC	7	0.70	22.47	0.67	22.74	2	0.59	19.98	0.61	19.48
SG**	2	0.99	4.44	0.99	4.47	1	0.99	2.69	0.99	2.66
SNV**	7	0.67	3.51	0.64	3.56	5	0.59	3.66	0.61	3.57

P1 = Pretreatment 1, Raw = Raw data, MV = Moving Average, GF = Gaussian Filter, MF = Median Filter, SG = Savitzky-Golay, SNV = Standard Normal Variate, SG* = Savitzky-Golay + Standard Normal Variate, B = Baseline, SG+B = Savitzky-Golay + Baseline, SNV* = Standard Normal Variate + Baseline, MSC = Multiplicative Scatter Correction, SG** = Savitzky-Golay + Multiplicative Scatter Correction, SNV** = Standard Normal Variate + Multiplicative Scatter Correction, respectively.

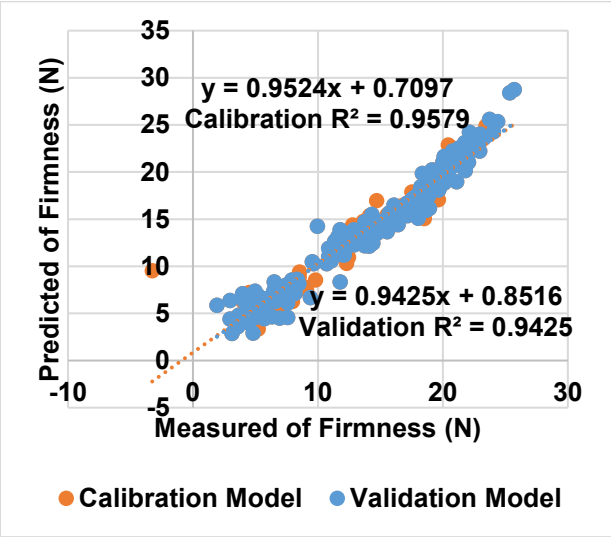

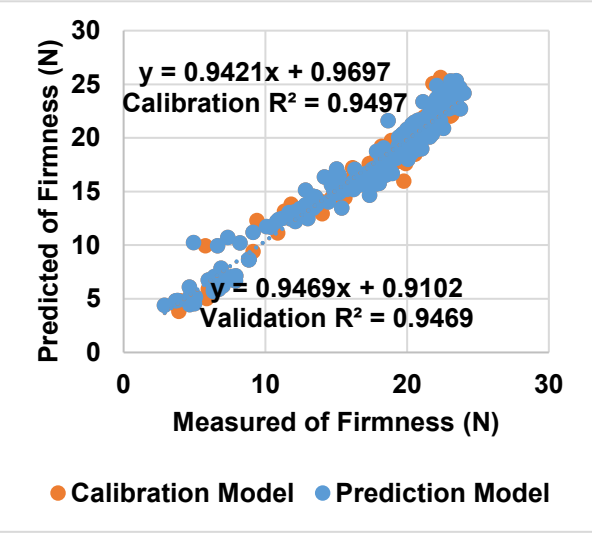

Fig. 13 Measured versus predicted healthy rind firmness at 12 weeks after anthesis from reflectance spectral data for calibration and validation models.

Fig. 14 Measured versus predicted bronzing-affected jackfruit rind firmness at 12 weeks after anthesis from reflectance spectral data for calibration and validation models.

Table 10 Performance of partial least squares regression (PLSR) models for predicting rind firmness of jackfruit cv. 'Tekam Yellow' at 14 weeks after anthesis using different Vis–NIR spectral preprocessing methods for calibration and validation datasets.

			Healthy Fruit					Bronzing-affected Fruit		
P1	**Lvs**	**Rv²**	**RMSEv**	**Rc²**	**RMSEc**	**Lvs**	**Rv²**	**RMSEv**	**Rc²**	**RMSEc**
Raw	7	0.30	21.12	0.28	21.81	7	0.27	28.15	0.28	28.85
MV	7	0.29	21.18	0.27	21.88	7	0.29	27.82	0.30	28.47
GF	7	0.30	17.73	0.28	18.29	7	0.26	24.12	0.26	24.72
MF	7	0.21	3.84	0.23	3.74	7	0.30	12.93	0.30	13.27
SG	7	0.36	7.54	0.34	7.67	7	0.33	12.95	0.34	13.32
SNV	7	0.48	3.49	0.49	3.93	7	0.41	5.00	0.41	5.09

SG*	**7**	**0.88**	**1.43**	**0.88**	**1.49**	**4**	**0.91**	**1.50**	**0.91**	**1.56**
B	7	0.32	21.19	0.30	21.86	7	0.44	25.65	0.44	26.34
SG+B	7	0.35	7.57	0.33	7.70	7	0.36	12.87	0.36	13.25
SNV*	7	0.38	4.19	0.36	4.35	7	0.48	4.79	0.49	4.86
MSC	7	0.44	19.68	0.43	20.50	7	0.42	25.05	0.42	25.65
SG**	7	0.86	7.09	0.83	7.99	4	0.97	3.43	0.97	3.47
SNV**	7	0.44	4.11	0.44	4.26	7	0.45	5.06	0.45	5.18

P1 = Pretreatment 1, Raw = Raw data, MV = Moving Average, GF = Gaussian Filter, MF = Median Filter, SG = Savitzky-Golay, SNV = Standard Normal Variate, SG* = Savitzky-Golay + Standard Normal Variate, B = Baseline, SG+B = Savitzky-Golay + Baseline, SNV* = Standard Normal Variate + Baseline, MSC = Multiplicative Scatter Correction, SG** = Savitzky-Golay + Multiplicative Scatter Correction, SNV** = Standard Normal Variate + Multiplicative Scatter Correction, respectively.

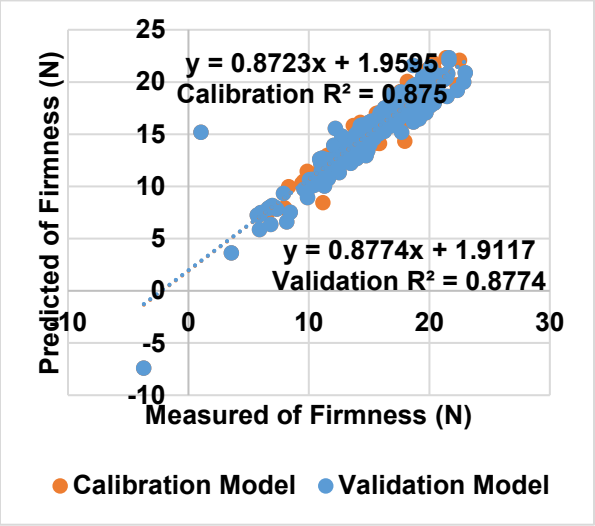

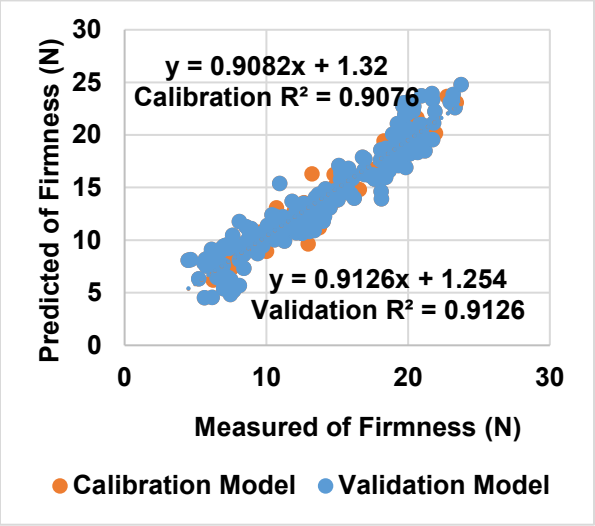

Fig. 15 Measured versus predicted healthy jackfruit rind firmness at 14 weeks after anthesis from reflectance spectral data for calibration and validation models.

Fig. 16 Measured versus predicted bronzing-affected jackfruit rind firmness at 14 weeks after anthesis from reflectance spectral data for calibration and validation models.

3.3.2 Predictive performance of PLSR models rind moisture content at 10 weeks after anthesis (WAA) and 14 weeks after anthesis (WAA)

Vis–NIR PLSR models provided reliable predictions of jackfruit rind moisture content at 10 and 14 weeks after anthesis (WAA) under optimized preprocessing strategies (Tables 11–12; Figs. 17–20).

At 10 WAA, healthy rind achieved the highest predictive accuracy using SNV followed by MSC with a single latent variable (LV), yielding $Rc^2 = 0.94$, RMSEc = 0.86, and $Rv^2 = 0.93$, RMSEv = 0.86. Bronzed rind performed best with SG+SNV and seven LVs, achieving $Rc^2 = 0.84$, RMSEc = 1.14, and $Rv^2 = 0.83$, RMSEv = 1.15 (Table 11). Although predictive precision was lower in bronzing-affected tissues, the models reliably captured moisture variation, reflecting underlying parenchymal water and carbohydrate dynamics [8]. Figures 17 and 18 show the measured versus predicted rind moisture content for healthy and bronzing-affected tissues, respectively.

At 14 WAA, healthy rind was modelled optimally with SNV+MSC and seven LVs ($Rc^2 = 0.97$, RMSEc = 0.68; $Rv^2 = 0.96$, RMSEv = 0.71), while bronzing-affected rind performed best using SG+SNV with four LVs ($Rc^2 = 0.82$, RMSEc = 1.38; $Rv^2 = 0.83$, RMSEv = 1.35) (Table 12). The high calibration–validation agreement for both fruit conditions demonstrates robust model performance despite spectral variability introduced by bronzing, confirming that Vis–NIR spectroscopy can accurately track rind moisture across maturity stages. Figures 19 and 20 illustrate measured versus predicted rind moisture at 14 WAA.

These results indicate that SNV+MSC provides a highly effective framework for predicting moisture in healthy rind, while SG+SNV with increased latent dimensionality remains suitable for bronzing-affected tissues. The findings are consistent with prior applications of Vis–NIR in fruit systems, where moisture and related compositional traits were successfully modelled for postharvest quality monitoring [4, 38, 51]. Collectively, these models confirm Vis–NIR spectroscopy as a rapid, non-destructive tool for monitoring rind hydration, supporting its integration into postharvest quality management and decision-making protocols for jackfruit supply chains.

Table 11 Performance of partial least squares regression (PLSR) models for predicting rind moisture content of jackfruit cv. 'Tekam Yellow' at 10 weeks after anthesis using different Vis–NIR spectral preprocessing methods for calibration and validation datasets.

			Healthy Fruit					Bronzing-affected Fruit		
P1	**Lvs**	**Rv²**	**RMSEv**	**Rc²**	**RMSEc**	**Lvs**	**Rv²**	**RMSEv**	**Rc²**	**RMSEc**
Raw	7	0.29	1.16	0.29	1.17	7	0.37	1.64	0.34	1.63
MV	6	0.14	5.58	0.16	5.35	7	0.17	6.27	0.19	6.32
GF	7	0.20	1.75	0.21	1.72	7	0.26	2.25	0.25	2.24
MF	6	0.14	16.15	0.17	15.44	7	0.18	16.28	0.19	15.97
SG	6	0.14	5.58	0.16	5.35	7	0.17	6.26	0.19	6.32
SNV	7	0.94	0.87	0.95	0.86	6	0.88	1.31	0.87	1.27
SG*	6	0.85	1.04	0.87	1.01	**7**	**0.83**	**1.15**	**0.82**	**1.14**
B	7	0.64	1.22	0.63	1.22	7	0.47	1.86	0.49	1.82
SG+B	7	0.16	5.47	0.18	5.27	7	0.15	6.32	0.17	6.36
SNV*	6	0.82	1.41	0.82	1.50	7	0.82	1.50	0.82	1.43
MSC	1	0.94	3.86	0.94	3.84	1	0.90	7.61	0.90	7.13
SG**	2	0.89	3.49	0.90	3.37	5	0.92	4.70	0.92	4.59
SNV**	**1**	**0.93**	**0.86**	**0.94**	**0.86**	2	0.85	1.51	0.84	1.40

P1 = Pretreatment 1, Raw = Raw data, MV = Moving Average, GF = Gaussian Filter, MF = Median Filter, SG = Savitzky-Golay, SNV = Standard Normal Variate, SG* = Savitzky-Golay + Standard Normal Variate, B = Baseline, SG+B = Savitzky-Golay + Baseline, SNV* = Standard Normal Variate + Baseline, MSC = Multiplicative Scatter Correction, SG** = Savitzky-Golay + Multiplicative Scatter Correction, SNV** = Standard Normal Variate + Multiplicative Scatter Correction, respectively.

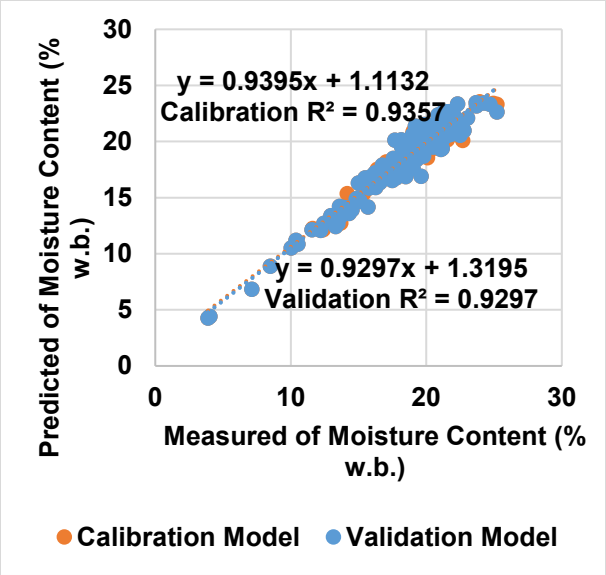

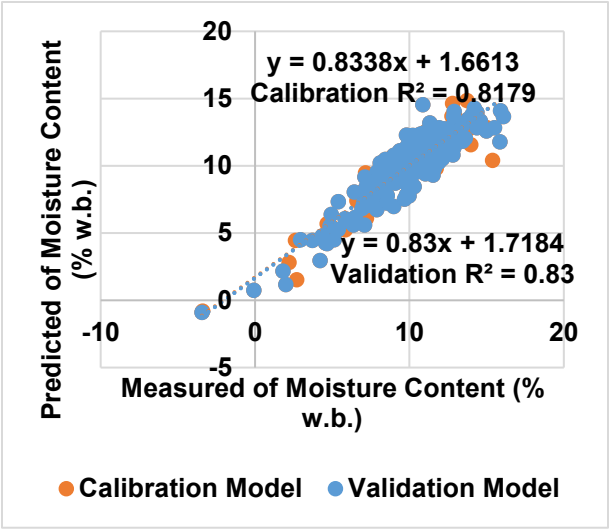

Fig. 17 Measured versus predicted healthy jackfruit rind moisture content at 10 weeks after anthesis from reflectance spectral data for calibration and validation models.

Fig. 18 Measured versus predicted bronzing-affected jackfruit rind moisture content at 10 weeks after anthesis from reflectance spectral data for calibration and validation models.

Table 12 Performance of partial least squares regression (PLSR) models for predicting rind moisture content of jackfruit cv. 'Tekam Yellow' at 12 weeks after anthesis using different Vis–NIR spectral preprocessing methods for calibration and validation datasets.

			Healthy Fruit					Bronzing-affected Fruit		
P1	**Lvs**	**Rv²**	**RMSEv**	**Rc²**	**RMSEc**	**Lvs**	**Rv²**	**RMSEv**	**Rc²**	**RMSEc**
Raw	7	0.22	2.75	0.23	2.58	3	0.97	4.41	0.97	4.63
MV	7	0.21	2.95	0.23	2.58	5	0.98	3.86	0.98	3.99
GF	7	0.22	3.25	0.24	3.07	4	0.95	4.73	0.94	4.85
MF	7	0.31	18.35	0.30	18.83	7	0.31	20.70	0.33	20.92
SG	7	0.26	7.23	0.24	7.36	6	0.24	9.65	0.25	9.94
SNV	7	0.89	1.26	0.89	1.29	3	0.89	2.09	0.89	2.10
SG*	7	0.78	1.33	0.78	1.37	**4**	**0.83**	**1.35**	**0.82**	**1.38**
B	7	0.34	2.83	0.37	2.66	4	0.96	5.00	0.96	5.20
SG+B	7	0.26	7.27	0.25	7.40	7	0.27	9.58	0.27	9.90
SNV*	7	0.61	2.17	0.58	2.34	7	0.90	2.01	0.90	2.01
MSC	6	0.92	5.40	0.92	1.55	4	0.90	9.90	0.90	10.00

SG**	7	0.83	5.55	0.81	5.99	3	0.83	5.40	0.83	5.53
SNV**	**7**	**0.96**	**0.71**	**0.97**	**0.68**	4	0.90	1.94	0.90	1.95

P1 = Pretreatment 1, Raw = Raw data, MV = Moving Average, GF = Gaussian Filter, MF = Median Filter, SG = Savitzky-Golay, SNV = Standard Normal Variate, SG* = Savitzky-Golay + Standard Normal Variate, B = Baseline, SG+B = Savitzky-Golay + Baseline, SNV* = Standard Normal Variate + Baseline, MSC = Multiplicative Scatter Correction, SG** = Savitzky-Golay + Multiplicative Scatter Correction, SNV** = Standard Normal Variate + Multiplicative Scatter Correction, respectively.

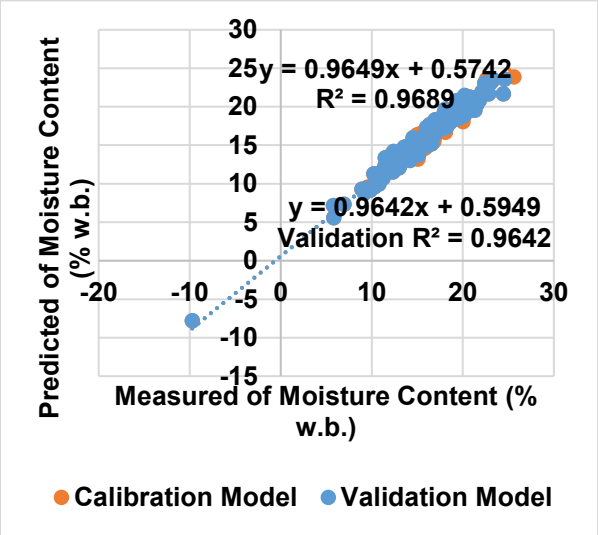

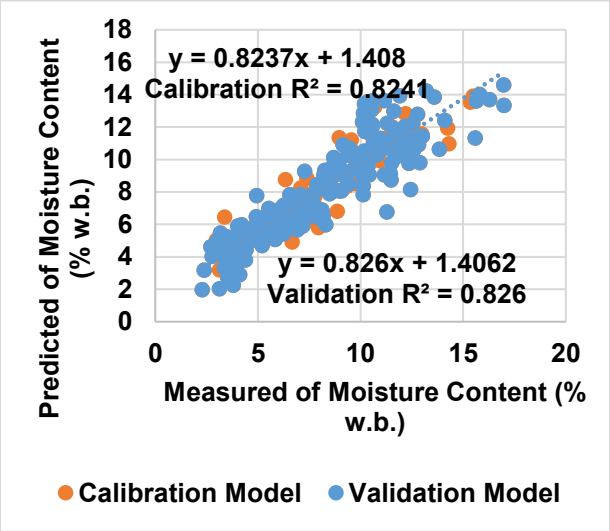

Fig. 19 Measured versus predicted healthy jackfruit rind moisture content at 14 weeks after anthesis from reflectance spectral data for calibration and validation models.

Fig. 20 Measured versus predicted bronzing-affected jackfruit rind moisture content at 14 weeks after anthesis from reflectance spectral data for calibration and validation models.

3.3.3 Predictive performance of PLSR models flesh moisture content at 12 weeks after anthesis (WAA) and 14 weeks after anthesis (WAA)

Vis–NIR PLSR models effectively predicted jackfruit flesh moisture content at 12 and 14 weeks after anthesis (WAA) under optimized spectral pretreatments (Tables 13–14; Figs. 21–24).

At 12 WAA, SG+SNV preprocessing provided the highest predictive accuracy for both healthy and bronzed flesh. Healthy tissue with five latent variables (LVs) achieved $Rc^2 = 0.98$, RMSEc = 0.78 and $Rv^2 = 0.98$, RMSEv = 0.76, while bronzed tissue with four LVs yielded $Rc^2 = 0.98$, RMSEc = 0.99 and $Rv^2 = 0.98$, RMSEv = 0.97 (Table 13). Figures 21 and 22 show the measured versus predicted values.

At 14 WAA, the same SG+SNV configuration with four LVs provided robust predictions. Healthy flesh achieved $Rc^2 = 0.96$, RMSEc = 1.17 and $Rv^2 = 0.95$, RMSEv = 1.15, whereas bronzed flesh reached $Rc^2 = 0.98$, RMSEc = 0.74 and $Rv^2 = 0.98$, RMSEv = 0.74 (Table 14; Figs. 23–24). The high calibration–validation agreement for both tissue types confirms strong model generalizability and minimal overfitting. The slightly higher accuracy in bronzing-affected tissues may reflect altered optical properties that enhance detection of water-related spectral features, consistent with observations in mandarin and potato [34, 38, 51].

These results demonstrate that SG+SNV is a robust, non-destructive approach for quantifying flesh moisture in jackfruit across mid- to late-maturity stages, supporting its application in postharvest monitoring, automated grading, and supply chain optimization.

Table 13 Performance of partial least squares regression (PLSR) models for predicting flesh moisture content of jackfruit cv. 'Tekam Yellow' at 12 weeks after anthesis using different Vis–NIR spectral preprocessing methods for calibration and validation datasets.

			Healthy Fruit					Bronzing-affected Fruit		
P1	**Lvs**	**Rv^2**	**RMSEv**	**Rc^2**	**RMSEc**	**Lvs**	**Rv^2**	**RMSEv**	**Rc^2**	**RMSEc**
Raw	7	0.44	2.45	0.41	2.48	1	0.39	3.46	0.41	3.40
MV	7	0.30	2.37	0.29	2.40	7	0.33	1.87	0.28	1.97
GF	7	0.40	2.09	0.37	2.12	7	0.49	2.56	0.50	2.50
MF	7	0.18	4.23	0.18	4.24	7	0.23	4.40	0.23	4.61
SG	7	0.30	2.37	0.29	2.40	7	0.33	1.87	0.28	1.97
SNV	2	0.93	1.80	0.93	1.77	5	0.92	1.94	0.92	1.96
SG*	**5**	**0.98**	**0.76**	**0.98**	**0.77**	**4**	**0.98**	**0.97**	**0.98**	**0.99**
B	7	0.42	2.44	0.40	2.47	7	0.39	3.44	0.41	3.38
SG+B	7	0.30	2.38	0.29	2.41	7	0.30	1.86	0.25	1.96
SNV*	3	0.93	1.71	0.93	1.69	7	0.91	1.88	0.91	1.88

MSC	2	0.96	6.95	0.97	6.88	1	0.96	6.70	0.96	6.93
SG**	3	0.99	3.18	0.99	3.31	1	0.99	2.25	0.99	2.29
SNV**	2	0.96	1.23	0.97	1.22	1	0.95	1.50	0.95	1.55

P1 = Pretreatment 1, Raw = Raw data, MV = Moving Average, GF = Gaussian Filter, MF = Median Filter, SG = Savitzky-Golay, SNV = Standard Normal Variate, SG* = Savitzky-Golay + Standard Normal Variate, B = Baseline, SG+B = Savitzky-Golay + Baseline, SNV* = Standard Normal Variate + Baseline, MSC = Multiplicative Scatter Correction, SG** = Savitzky-Golay + Multiplicative Scatter Correction, SNV** = Standard Normal Variate + Multiplicative Scatter Correction, respectively.

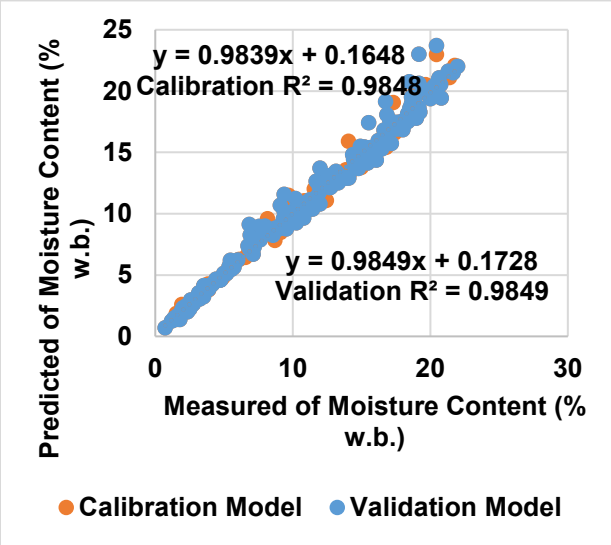

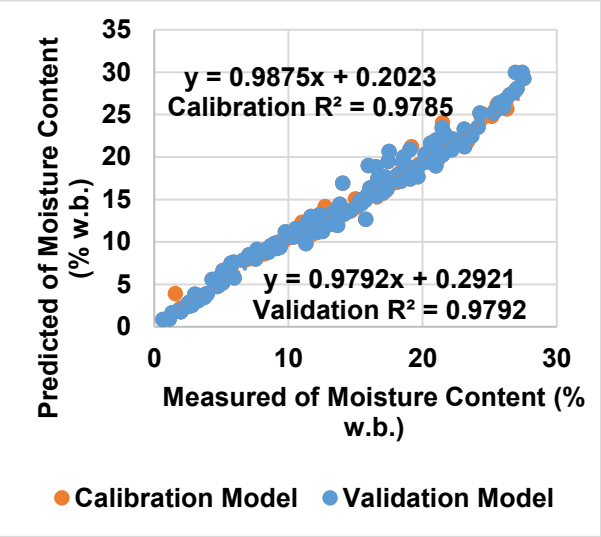

Fig. 21 Measured versus predicted healthy jackfruit flesh moisture content at 12 weeks after anthesis from reflectance spectral data for calibration and validation models.

Fig. 22 Measured versus predicted bronzing-affected jackfruit flesh moisture content at 12 weeks after anthesis from reflectance spectral data for calibration and validation models.

Table 14 Performance of partial least squares regression (PLSR) models for predicting flesh moisture content of jackfruit cv. 'Tekam Yellow' at 14 weeks after anthesis using different Vis–NIR spectral preprocessing methods for calibration and validation datasets.

			Healthy Fruit					Bronzing-affected Fruit		
P1	**Lvs**	**Rv²**	**RMSEv**	**Rc²**	**RMSEc**	**Lvs**	**Rv²**	**RMSEv**	**Rc²**	**RMSEc**
Raw	1	0.00	4.78	0.00	4.80	7	0.16	6.77	0.14	7.28
MV	4	0.95	2.11	0.95	2.05	6	0.66	1.58	0.70	1.59
GF	1	0.21	3.63	0.20	3.65	7	0.60	3.87	0.62	4.03
MF	4	0.63	7.42	0.63	7.30	6	0.20	4.92	0.19	5.02
SG	4	0.95	2.11	0.95	2.05	6	0.66	1.58	0.70	1.59
SNV	7	0.90	2.71	0.91	2.65	3	0.88	2.31	0.88	2.35

SG*	**4**	**0.95**	**1.15**	**0.96**	**1.17**	**4**	**0.98**	**0.74**	**0.98**	**0.74**
B	1	0.99	7.73	0.99	7.58	7	0.16	6.75	0.15	7.26
SG+B	1	0.99	4.69	0.99	4.55	6	0.69	1.60	0.72	1.61
SNV*	4	0.89	2.32	0.89	2.28	6	0.90	2.06	0.89	2.13
MSC	2	0.99	NS	0.99	NS	2	0.99	3.01	0.99	3.12
SG**	2	0.99	NS	0.98	NS	2	0.99	1.81	0.99	1.79
SNV**	6	0.98	1.20	0.98	1.19	2	0.99	0.83	0.99	0.85

P1 = Pretreatment 1, Raw = Raw data, MV = Moving Average, GF = Gaussian Filter, MF = Median Filter, SG = Savitzky-Golay, SNV = Standard Normal Variate, SG* = Savitzky-Golay + Standard Normal Variate, B = Baseline, SG+B = Savitzky-Golay + Baseline, SNV* = Standard Normal Variate + Baseline, MSC = Multiplicative Scatter Correction, SG** = Savitzky-Golay + Multiplicative Scatter Correction, SNV** = Standard Normal Variate + Multiplicative Scatter Correction, respectively.

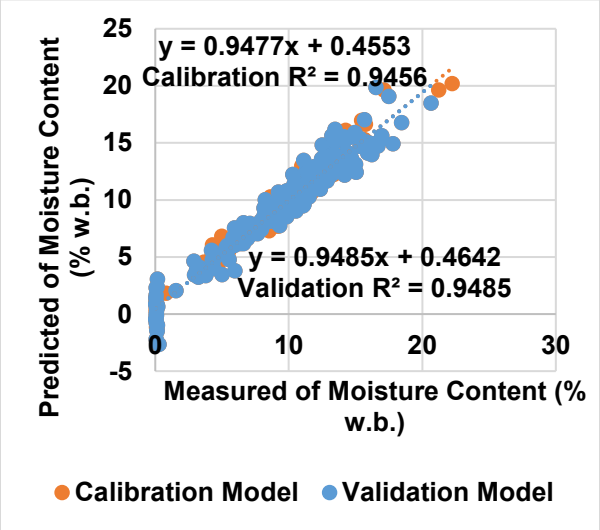

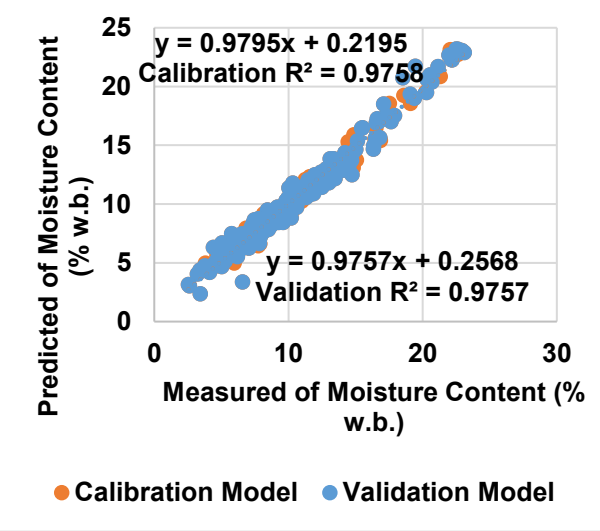

Fig. 23 Measured versus predicted healthy jackfruit flesh moisture content at 14 weeks after anthesis from reflectance spectral data for calibration and validation models.
Fig. 24 Measured versus predicted bronzing-affected jackfruit flesh moisture content at 14 weeks after anthesis from reflectance spectral data for calibration and validation models.

3.3.4 Predictive performance of PLSR models seed moisture content at 10 weeks after anthesis (WAA), 12 weeks after anthesis (WAA) and 14 weeks after anthesis (WAA)

Vis–NIR PLSR models reliably predicted jackfruit seed moisture content at 10, 12, and 14 weeks after anthesis (WAA) under optimized spectral pretreatments (Tables 15–17; Figs. 25–30).

At 10 WAA, the SG+MSC configuration with three latent variables (LVs) provided the best performance for healthy seeds, achieving $Rc^2 = 0.99$, RMSEc = 0.46 and $Rv^2 = 0.99$, RMSEv = 0.47. For bronzed seeds, SG+SNV with four LVs yielded $Rc^2 = 0.96$, RMSEc = 0.99 and $Rv^2 = 0.96$, RMSEv = 1.07 (Table 15; Figs. 25–26).

At 12 WAA, SG+SNV preprocessing was optimal for both healthy (five LVs; $Rc^2 = 0.98$, RMSEc = 0.95; $Rv^2 = 0.97$, RMSEv = 0.98) and bronzed seeds (four LVs; $Rc^2 = 0.97$, RMSEc = 1.04; $Rv^2 = 0.97$, RMSEv = 1.06) (Table 16; Figs. 27–28).

At 14 WAA, SG+SNV with four LVs provided consistent and high predictive accuracy. Healthy seeds achieved $Rc^2 = 0.94$, RMSEc = 1.25 and $Rv^2 = 0.94$, RMSEv = 1.25, while bronzed seeds reached $Rc^2 = 0.97$, RMSEc = 0.85 and $Rv^2 = 0.97$, RMSEv = 0.87 (Table 17; Figs. 29–30).

Across all stages, calibration–validation alignment was strong, confirming model robustness and minimal overfitting. The slightly superior accuracy in bronzing-affected tissues may reflect altered optical properties that enhance water-related spectral feature detection, consistent with prior studies in other fruit systems [34, 37, 38, 45, 51].

These results demonstrate that SG+MSC or SG+SNV preprocessing provides a robust, non-destructive framework for seed moisture prediction during early to late maturity, supporting applications in postharvest monitoring, seed quality evaluation, and germplasm conservation.

Table 15 Performance of partial least squares regression (PLSR) models for predicting seed moisture content of jackfruit cv. 'Tekam Yellow' at 10 weeks after anthesis using different Vis–NIR spectral preprocessing methods for calibration and validation datasets.

			Healthy Fruit					Bronzing-affected Fruit		
P1	**Lvs**	**Rv^2**	**RMSEv**	**Rc^2**	**RMSEc**	**Lvs**	**Rv^2**	**RMSEv**	**Rc^2**	**RMSEc**
Raw	1	0.00	46.67	0.00	53.75	7	0.22	5.73	0.23	5.69

MV	2	0.99	1.54	0.99	1.54	7	0.51	3.05	0.54	2.88
GF	3	0.99	4.42	0.99	4.49	7	0.74	2.86	0.73	2.93
MF	2	0.04	6.44	0.04	6.75	6	0.16	6.36	0.16	6.04
SG	2	0.99	1.54	0.99	1.54	7	0.51	3.05	0.54	2.88
SNV	7	0.95	1.30	0.96	1.27	7	0.87	1.73	0.87	1.75
SG*	3	0.97	1.09	0.97	1.08	**4**	**0.96**	**1.07**	**0.96**	**0.99**
B	2	0.35	5.33	0.43	5.23	7	0.27	5.68	0.31	5.53
SG+B	7	0.78	1.21	0.79	1.22	7	0.53	3.05	0.55	2.88
SNV*	7	0.86	1.60	0.86	1.61	7	0.82	1.98	0.80	2.04
MSC	7	0.75	16.60	0.77	17.83	2	0.90	5.97	0.91	5.73
SG**	**3**	**0.99**	**0.47**	**0.99**	**0.46**	2	0.99	1.71	0.99	1.65
SNV**	7	0.70	4.72	0.72	5.14	2	0.89	1.71	0.89	1.63

P1 = Pretreatment 1, Raw = Raw data, MV = Moving Average, GF = Gaussian Filter, MF = Median Filter, SG = Savitzky-Golay, SNV = Standard Normal Variate, SG* = Savitzky-Golay + Standard Normal Variate, B = Baseline, SG+B = Savitzky-Golay + Baseline, SNV* = Standard Normal Variate + Baseline, MSC = Multiplicative Scatter Correction, SG** = Savitzky-Golay + Multiplicative Scatter Correction, SNV** = Standard Normal Variate + Multiplicative Scatter Correction, respectively.

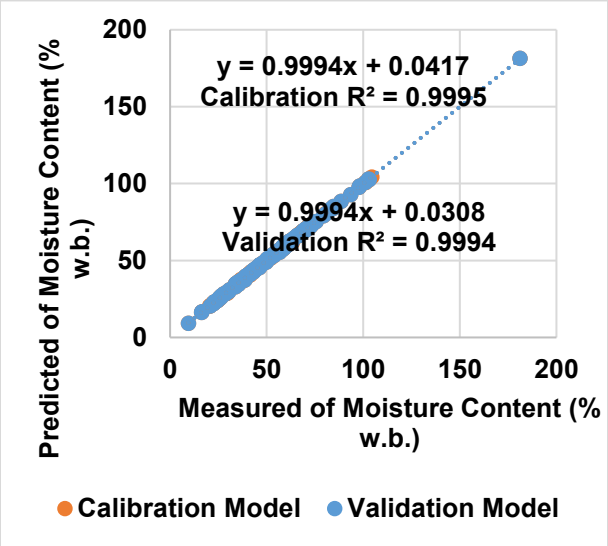

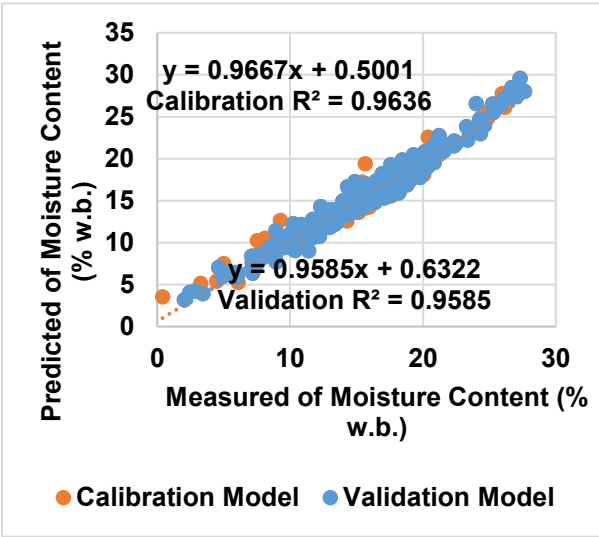

Fig. 25 Measured versus predicted healthy jackfruit seed moisture content at 10 weeks after anthesis from reflectance spectral data for calibration and validation models.

Fig. 26 Measured versus predicted bronzing-affected jackfruit seed moisture content at 10 weeks after anthesis from reflectance spectral data for calibration and validation models.

Table 16 Performance of partial least squares regression (PLSR) models for predicting seed moisture content of jackfruit cv. 'Tekam Yellow' at 12 weeks after anthesis using different Vis–NIR spectral preprocessing methods for calibration and validation datasets.

			Healthy Fruit					Bronzing-affected Fruit		
P1	**Lvs**	**Rv²**	**RMSEv**	**Rc²**	**RMSEc**	**Lvs**	**Rv²**	**RMSEv**	**Rc²**	**RMSEc**
Raw	7	0.18	6.45	0.16	6.46	7	0.26	6.31	0.28	6.20
MV	7	0.64	2.25	0.63	2.30	7	0.60	2.00	0.56	2.11
GF	7	0.58	3.92	0.56	3.96	7	0.71	3.28	0.71	3.27
MF	7	0.17	6.04	0.15	6.18	7	0.26	5.72	0.26	5.78
SG	7	0.64	2.25	0.63	2.30	7	0.60	2.00	0.56	2.11
SNV	3	0.92	1.76	0.92	1.77	7	0.91	1.93	0.90	2.00
SG*	**5**	**0.97**	**0.98**	**0.98**	**0.95**	**4**	**0.97**	**1.06**	**0.97**	**1.04**
B	7	0.19	6.44	0.17	6.45	7	0.25	6.33	0.27	6.20
SG+B	7	0.65	2.25	0.64	2.30	7	0.59	1.99	0.54	2.11
SNV*	3	0.91	1.81	0.91	1.80	7	0.88	2.09	0.87	2.16
MSC	3	0.95	7.72	0.95	7.42	1	0.95	7.77	0.94	7.93
SG**	3	0.98	3.98	0.98	3.98	1	0.99	2.79	0.99	2.85
SNV**	2	0.93	1.53	0.94	1.49	1	0.93	1.73	0.93	1.77

P1 = Pretreatment 1, Raw = Raw data, MV = Moving Average, GF = Gaussian Filter, MF = Median Filter, SG = Savitzky-Golay, SNV = Standard Normal Variate, SG* = Savitzky-Golay + Standard Normal Variate, B = Baseline, SG+B = Savitzky-Golay + Baseline, SNV* = Standard Normal Variate + Baseline, MSC = Multiplicative Scatter Correction, SG** = Savitzky-Golay + Multiplicative Scatter Correction, SNV** = Standard Normal Variate + Multiplicative Scatter Correction, respectively.

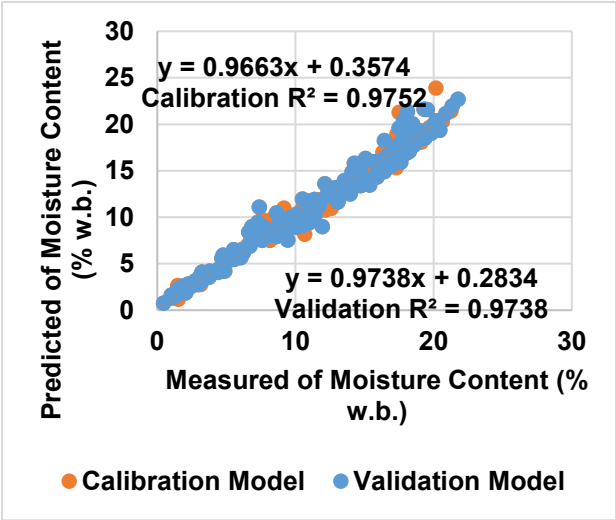

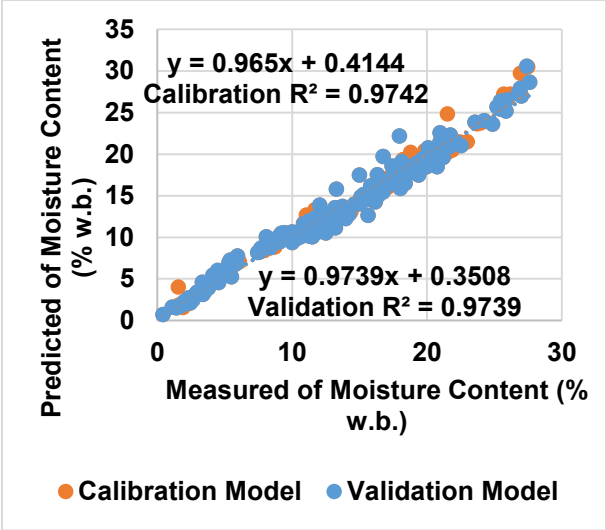

Fig. 27 Measured versus predicted healthy jackfruit seed moisture content at 12 weeks after anthesis from reflectance spectral data for calibration and validation models.

Fig. 28 Measured versus predicted bronzing-affected jackfruit seed moisture content at 12 weeks after anthesis from reflectance spectral data for calibration and validation models.

Table 17 Performance of partial least squares regression (PLSR) models for predicting seed moisture content of jackfruit cv. 'Tekam Yellow' at 14 weeks after anthesis using different Vis–NIR spectral preprocessing methods for calibration and validation datasets.

			Healthy Fruit					Bronzing-affected Fruit		
P1	**Lvs**	**Rv²**	**RMSEv**	**Rc²**	**RMSEc**	**Lvs**	**Rv²**	**RMSEv**	**Rc²**	**RMSEc**
Raw	2	0.06	10.59	0.07	10.56	7	0.31	9.36	0.28	9.41
MV	4	0.85	3.49	0.85	3.50	6	0.82	1.50	0.82	4.87
GF	7	0.05	8.42	0.04	8.43	7	0.80	4.17	0.79	4.21
MF	3	0.38	7.44	0.36	7.42	6	0.22	4.66	0.22	4.67
SG	4	0.85	3.49	0.85	3.50	6	0.82	1.50	0.82	1.49
SNV	7	0.89	2.87	0.89	2.87	2	0.86	2.51	0.86	2.54
SG*	**4**	**0.94**	**1.25**	**0.94**	**1.25**	**4**	**0.97**	**0.87**	**0.97**	**0.85**
B	1	0.99	12.81	0.99	12.90	7	0.30	9.21	0.26	9.28
SG+B	1	0.99	5.72	0.99	5.89	6	0.80	1.51	0.79	1.50
SNV*	5	0.89	2.54	0.89	2.47	6	0.88	2.19	0.87	2.27
MSC	2	0.99	NS	0.99	NS	2	0.98	4.02	0.98	4.10
SG**	1	0.99	NS	0.99	NS	1	0.98	2.70	0.97	2.70

SNV**	6	0.96	1.52	0.96	1.53	2	0.98	1.11	0.97	1.13

P1 = Pretreatment 1, Raw = Raw data, MV = Moving Average, GF = Gaussian Filter, MF = Median Filter, SG = Savitzky-Golay, SNV = Standard Normal Variate, SG* = Savitzky-Golay + Standard Normal Variate, B = Baseline, SG+B = Savitzky-Golay + Baseline, SNV* = Standard Normal Variate + Baseline, MSC = Multiplicative Scatter Correction, SG** = Savitzky-Golay + Multiplicative Scatter Correction, SNV** = Standard Normal Variate + Multiplicative Scatter Correction, respectively.

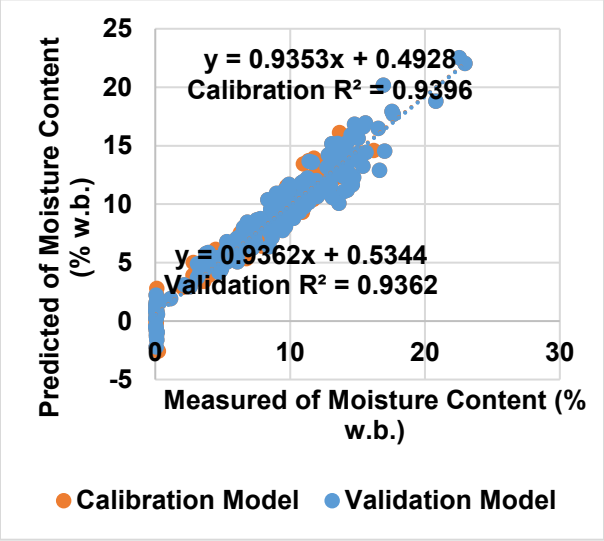

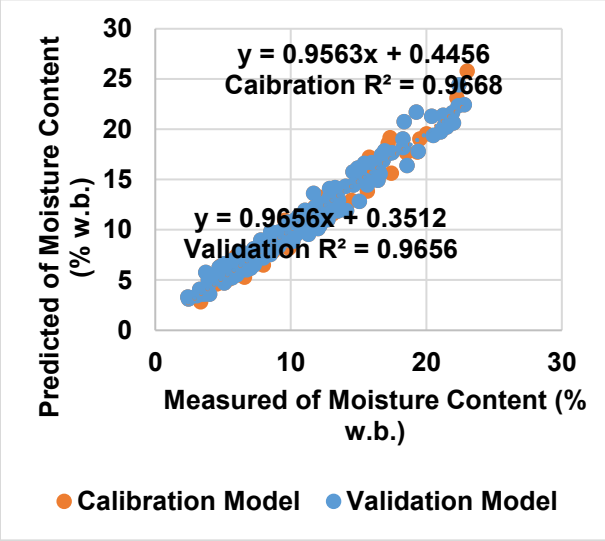

Fig. 29 Measured versus predicted healthy jackfruit seed moisture content at 14 weeks after anthesis from reflectance spectral data for calibration and validation models.

Fig. 30 Measured versus predicted bronzing-affected jackfruit seed moisture content at 14 weeks after anthesis from reflectance spectral data for calibration and validation models.

3.3.5 PLS-Based prediction of rind, flesh, and seed quality in jackfruit across maturity stages and fruit conditions

The predictive strength of Partial Least Squares (PLS) models in estimating key jackfruit quality parameters—namely rind firmness, flesh firmness, and moisture content of rind, flesh, and seed—was assessed across three maturity stages (10, 12, and 14 WAA) and under two fruit conditions (healthy and bronzed). The summary statistics for these models are presented in Tables 18 to 21.

These findings affirm that Vis-NIR spectroscopy, when integrated with suitable PLS modeling and spectral preprocessing, can offer robust, non-destructive estimations of key postharvest quality indicators in jackfruit. High RPD values (especially >3.0) validate the quantitative reliability of

657 the models [15, 46], while minimal bias and strong correlations support their deployment in
658 commercial quality control frameworks.

659 This reinforces the recommendation by [34]. to assess model validity through a suite of metrics—
660 including Rp^2, RMSEP, bias, and RPD—to ensure comprehensive evaluation of predictive
661 performance. The fidelity of these models across health statuses and developmental stages also
662 suggests potential for broader generalizability, provided that representative calibration datasets are
663 established [13, 52].

664 For fruit prediction models, RPD values below 1.5 are deemed unusable, RPD values between 1.5
665 and 2.0 are appropriate for approximate predictions, RPD values between 2.0 and 2.5 are
666 appropriate for quantitative predictions, and most RPD values between 2.5 and 3.0 and above are
667 regarded as good and excellent prediction models, according to [15, 46]. As per the findings of
668 [34], the RPD values for the majority of the carbohydrates' models were higher than 1.5 but lower
669 than 2.0, and the correlation between the Vis/NIRS predicted and observed values was medically
670 acceptable ($r > 0.70$). As a result, the highlights the significance of assessing calibration and
671 prediction model performance utilizing a mix of statistical characteristics in order to forecast the
672 jackfruit quality features.

673 Prediction models based on a single orchard population for bronzing-affected flesh moisture
674 content also showed a considerable absolute bias of up to 0.03 (Table 20) in 12 WAA. The greater
675 bias of the carbohydrate models, according to [34], showed that the models were not stable and
676 that external factors, such the location of the orchard, would have an impact. The fact that the data
677 from the measured validation set from the orchard was not contained within the data from the
678 measured calibration set may have contributed to the reduced prediction accuracy for rind firmness

models for bronzing 10 WAA. Most calibration models developed from an orchard population violated a general rule of thumb that states that samples used to build a calibration or prediction model should be samples that are similar to or same as those that will be measured during validation or analysis in the future [13, 52].

Table 18: Summary of principal results obtained in the PLS models effects of healthiness and maturity stages (weeks after anthesis) on rind firmness of jackfruit cv. 'Tekam Yellow'.

Healthiness	Weeks	LVs	Rc^2	RMSEc	Rp^2	RMSEp	Bias	Slope	Offset	Correlation	RPD
Normal	10	6	0.95	0.93	0.95	0.94	0.02	0.94	1.07	0.97	19.20
Bronzing	10	7	0.94	1.03	0.93	1.06	-0.05	0.94	0.96	0.96	19.21
Normal	12	3	0.94	1.50	0.96	1.29	0.00	0.95	0.71	0.98	19.30
Bronzing	12	5	0.95	1.23	0.95	1.18	-0.02	0.94	0.97	0.97	18.60
Normal	14	7	0.88	1.43	0.87	1.49	-0.02	0.87	1.96	0.94	17.08
Bronzing	14	4	0.91	1.50	0.91	1.56	0.00	0.91	1.32	0.95	20.58

Table 19: Summary of principal results obtained in the PLS models effects of healthiness and maturity stages (weeks after anthesis) on rind moisture content of jackfruit cv. 'Tekam Yellow'.

Healthiness	Weeks	LVs	Rc^2	RMSEc	Rp^2	RMSEp	Bias	Slope	Offset	Correlation	RPD
Normal	10	7	0.94	0.87	0.95	0.86	-0.03	0.94	1.08	0.98	1.62
Bronzing	10	7	0.83	1.15	0.82	1.14	-0.02	0.83	1.66	0.9	1.82
Normal	14	7	0.96	0.71	0.97	0.68	-0.01	0.96	0.57	0.98	4.60
Bronzing	14	4	0.83	1.35	0.82	1.37	-0.02	0.82	1.41	0.91	3.18

Table 20: Summary of principal results obtained in the PLS models effects of healthiness and maturity stages (weeks after anthesis) on flesh moisture content of jackfruit cv. 'Tekam Yellow'.

Healthiness	Weeks	LVs	Rc^2	RMSEc	Rp^2	RMSEp	Bias	Slope	Offset	Correlation	RPD
Normal	12	5	0.98	0.76	0.98	0.77	-0.02	0.98	0.16	0.99	4.30
Bronzing	12	4	0.98	0.97	0.98	0.99	0.03	0.99	0.2	0.99	4.51

Normal	14	4	0.95	1.15	0.95	1.16	-0.02	0.95	0.46	0.97	4.22
Bronzing	14	4	0.98	0.74	0.98	0.74	0.01	0.98	0.22	0.99	10.16

Table 21: Summary of principal results obtained in the PLS models effects of healthiness and maturity stages (weeks after anthesis) on seed moisture content of jackfruit cv. 'Tekam Yellow'.

Healthiness	Weeks	LVs	Rc^2	RMSEc	Rp^2	RMSEp	Bias	Slope	Offset	Correlation	RPD
Normal	10	3	0.99	0.47	0.99	0.46	0.01	1.00	0.04	1.00	12.29
Bronzing	10	4	0.96	1.07	0.96	0.99	-0.01	0.97	0.50	0.98	6.61
Normal	12	5	0.97	0.98	0.98	0.95	-0.01	0.97	0.36	0.99	7.64
Bronzing	12	4	0.97	1.06	0.97	1.04	-0.05	0.97	0.41	0.99	7.26
Normal	14	4	0.94	1.25	0.94	1.25	-0.06	0.94	0.49	0.97	8.81
Bronzing	14	4	0.97	0.87	0.97	0.85	0.00	0.96	0.45	0.98	8.88

4. Discussion

The progressive reduction in jackfruit (*Artocarpus heterophyllus*) flesh firmness—from 334.01 N at 10 weeks after anthesis (WAA) to 136.74 N at 14 WAA—corresponds with known ripening-related biochemical processes, particularly the enzymatic depolymerization of pectin and hemicellulose mediated by polygalacturonase, cellulase, and β-galactosidase [41]. Such softening dynamics are characteristic of climacteric fruit physiology and serve as key indices for determining harvest maturity [44, 48].

Interestingly, bronzing-affected jackfruit exhibited anomalously higher firmness values at both 10 and 14 WAA. This could be attributed to physiological responses induced by jackfruit bronzing disease (JBD), such as lignin or callose deposition, which reinforce cell wall rigidity and impede normal enzymatic disassembly [27]. Alternatively, the retention of free water in intercellular

spaces—potentially caused by cellular disruption—may yield artificially elevated firmness readings, a phenomenon previously observed in tropical fruits under abiotic stress [14]. These findings suggest a dual mechanism wherein both structural fortification and abnormal water distribution contribute to altered firmness patterns in diseased tissues, consistent with pathophysiological disruptions observed in postharvest fruit disorders [50]. Similar alterations in rind and flesh characteristics associated with bronzing disorder have previously been reported in jackfruit, indicating that the disease substantially modifies tissue structure and physical quality attributes across different stages of fruit development [30].

Water dynamics in the rind, flesh, and seed tissues revealed substantial variability in response to both maturation and bronzing-induced stress. In healthy fruit, flesh moisture content increased from 69.19% at 10 WAA to 72.62% at 14 WAA, which aligns with expected physiological changes such as starch hydrolysis, cell expansion, and solute accumulation [25, 33]. The rind, acting as a protective barrier, maintained relatively stable moisture levels, underscoring its role in water retention and fruit integrity. Conversely, bronzing-affected tissues—particularly in seeds and flesh—exhibited elevated moisture levels, notably at 12 and 14 WAA. This abnormal accumulation likely reflects disease-mediated disruptions in water regulation, including compromised membrane function, impaired aquaporin activity, and osmoregulatory failure [9, 29]. Such anomalies not only influence fruit texture and microbial susceptibility but also impact physiological viability, particularly in seeds where moisture imbalance can impair desiccation tolerance and germination potential [49]. These observations are consistent with previous reports showing that bronzing disorder induces substantial alterations in the physical characteristics of jackfruit tissues during fruit development, suggesting that disease-related structural modifications may also influence water distribution and retention within affected tissues [30].

Firmness loss in both rind and flesh followed a typical ripening trajectory in healthy fruit, with values declining progressively from 10 to 14 WAA. However, bronzing accelerated this softening process. For example, flesh firmness in bronzed samples declined from 18.3 N at 10 WAA to 6.2 N at 14 WAA—exceeding the rate of decline observed in healthy controls. This pattern was paralleled in rind firmness, which although consistently higher than flesh, also deteriorated more rapidly under bronzing conditions. These findings implicate microbial and enzymatic activity in hastening textural breakdown in diseased fruit, likely through disruption of polysaccharide networks and tissue turgor [18, 46].

The performance of partial least squares regression (PLSR) models using Vis-NIR spectroscopy was generally robust. For firmness prediction, calibration models yielded R^2 values above 0.91 for both flesh and rind, with root mean square error of calibration (RMSEC) values of 0.64 N and 0.82 N, respectively. The ratio of performance to deviation (RPD) values exceeded 2.5, indicating strong predictive utility [15, 46]. These results affirm the effectiveness of Vis-NIR spectroscopy in non-destructive firmness monitoring and support its application for large, heterogeneous fruits such as jackfruit where internal variability limits traditional sampling approaches [10, 18]. The predictive performance achieved in the present study is comparable to previous Vis–NIR applications in jackfruit, where soluble solids concentration and ascorbic acid were successfully estimated from spectral information acquired from intact fruit tissues, confirming the suitability of Vis–NIR spectroscopy for non-destructive assessment of multiple jackfruit quality attributes [31].

Regarding moisture content, PLSR models demonstrated tissue-specific accuracy. In flesh, the model exhibited excellent performance ($R^2 = 0.93$; RMSEP = 1.82%; RPD = 2.9), while rind and seed models were moderately predictive (RPD = 2.4 and 1.8, respectively). These outcomes are

consistent with the optical properties of these tissues, where the higher heterogeneity and light-scattering characteristics of rind and seeds reduce spectral signal stability [34, 37].

Due to the limited optical penetration depth of Vis–NIR radiation within the 500–950 nm region, the obtained spectra primarily reflected combined information related to rind structure, water distribution, tissue scattering, and physiological changes that were indirectly associated with internal flesh and seed properties. Therefore, the predictive capability of the developed models should be interpreted primarily as correlation-based rather than direct biochemical detection, consistent with previous studies highlighting the indirect, multivariate nature of Vis–NIR prediction in heterogeneous fruit matrices [40, 41].

The developed Vis–NIR models demonstrated strong predictive capability; however, the observed spectral responses likely reflected complex interactions among water distribution, tissue structure, scattering behavior, pigment variation, and physiological disorder progression rather than direct detection of specific biochemical constituents. Spectral responses associated with moisture variation within the analyzed spectral range were important for capturing tissue water dynamics and physiological changes related to fruit maturation and bronzing disorder. This interpretation is consistent with recent reviews highlighting that Vis–NIR spectroscopy primarily captures integrated spectral responses arising from multiple physical and biochemical attributes, particularly in heterogeneous fruit tissues where water status, structural characteristics, and optical scattering collectively influence model performance [32].

Moisture losses in bronzed samples deviated from the gradual trends observed in healthy tissues, particularly at 12 and 14 WAA. Abnormal reductions in flesh and seed moisture suggest structural compromise and loss of membrane integrity, resulting in impaired water retention. These

physiological changes were well captured in the Vis-NIR spectra and are reflective of bronzing-induced senescence or pathogen infiltration. Notably, the performance of seed moisture models was lower, reflecting the need for optimized pretreatment strategies and calibration models that account for anatomical complexities, including seed coat thickness and internal compartmentalization [34].

Importantly, the current findings are in line with prior studies on apple, peach, and kiwifruit, which also report that prediction model robustness is influenced by cultivar, maturity stage, and growing environment [22, 24, 40, 43]. As with other climacteric fruits, the biological variability of jackfruit—amplified by bronzing pathology—necessitates multivariate calibration strategies and cross-environmental validation to ensure model generalizability.

Overall, this study affirms the potential of Vis-NIR spectroscopy, coupled with advanced spectral pretreatment (e.g., Savitzky-Golay and SNV), for real-time, non-destructive estimation of moisture content and firmness in jackfruit. The integration of disease differentiation (normal vs. bronzed) and developmental profiling (10–14 WAA) provides a nuanced understanding of fruit quality evolution and supports the deployment of Vis-NIR systems in postharvest management and quality assurance workflows.

5. Conclusions

Malaysia's thriving jackfruit industry plays a significant economic role, supporting both domestic markets and export sectors. However, the emergence of jackfruit bronzing disease (JBD), associated with *Pantoea stewartii*, poses a serious phytopathological and economic threat. The disease affects fruit quality, reduces marketability, and may compromise regional agricultural

sustainability and trade competitiveness. Therefore, improved understanding of its physiological impact and reliable, rapid detection approaches are essential.

This study demonstrates the effectiveness of visible–near infrared (Vis–NIR) spectroscopy combined with partial least squares regression (PLSR) for non-destructive prediction of key quality attributes, particularly firmness and moisture content, across rind, flesh, and seed tissues of jackfruit (*Artocarpus heterophyllus* cv. 'Tekam Yellow'). Firmness showed a consistent decline from 10 to 14 weeks after anthesis (WAA), with bronzing-affected fruit exhibiting more pronounced tissue softening compared with healthy fruit. These changes were successfully captured by Vis–NIR-based predictive models, which achieved strong performance, with R^2 values generally exceeding 0.91 and high residual predictive deviation (RPD), particularly for flesh firmness.

Moisture content exhibited clear tissue-dependent behaviour, with flesh and rind showing more stable and interpretable spectral–physiological relationships, whereas seed moisture prediction was comparatively less robust due to higher structural density and stronger light scattering effects. Overall, the developed models were able to describe the general trends of moisture variation during maturation and bronzing progression, although predictive performance varied across tissues and developmental stages.

Collectively, these findings confirm the potential of Vis–NIR spectroscopy as a rapid, non-destructive and real-time approach for assessing internal physiological quality and detecting disorder-related changes in jackfruit. The integration of such spectral techniques into postharvest handling systems and quality grading workflows could support early identification of bronzing symptoms and improve decision-making for sorting and market distribution.

Despite the promising predictive performance obtained in this study, several limitations should be acknowledged. The models were developed using samples collected from a single orchard and one harvest season, which may limit their generalizability under broader agro-climatic and management conditions. In addition, external validation using independent datasets from different orchards, seasons, and potentially different cultivars was not performed. Future research should therefore focus on expanding dataset diversity, incorporating multi-season and multi-location validation, and integrating additional physicochemical quality parameters such as soluble solids content, sugar composition, and acidity. The application of advanced machine learning and deep learning approaches may further enhance prediction accuracy and model robustness for industrial-scale deployment.

To mitigate the impact of JBD, a comprehensive strategy is required, including continued research investment, development of resistant cultivars, and adoption of precision agriculture technologies such as Vis–NIR spectroscopy. Strengthening collaboration among researchers, growers, industry stakeholders, and policy makers will be essential to improve disease management, safeguard fruit quality, and enhance the resilience of the jackfruit supply chain in Malaysia.

Author Contributions Declaration

Conceptualization, **Kok Jeng Lim**, **Phebe Ding**, and **Nazmi Mat Nawi**; Literature review and data collection, **Kok Jeng Lim**; Writing – original draft, **Kok Jeng Lim**; Writing – review and editing, **Phebe Ding**, **Nazmi Mat Nawi**, and **Mashitah Jusoh**; Supervision, **Phebe Ding**, **Nazmi Mat Nawi**, and **Mashitah Jusoh**. Funding acquisition: not applicable.

Data Availability Declaration

The datasets generated during and/or analyzed during the current study are available.

Funding Declaration

This research did not receive any specific grant from funding agencies in the public, commercial, or not-for-profit sectors.

Declaration of Completing Interest

The authors declare that they have no completing financial interests or personal relationships that could have appeared to influence the work reported in this paper.

Declaration of Ethical Approval

Not applicable.

Declaration of Consent to Participate

Not applicable.

Declaration of Consent for Publication

Not applicable.

Acknowledgements

The authors gratefully acknowledge the technical and logistical support provided by the Department of Crop Science, Faculty of Agriculture; the Department of Biological and Agricultural Engineering, Faculty of Engineering; and the Institute of Plantation Studies, Universiti Putra Malaysia.

References

[1] Abdullah, N., Nawi, N. M., Ding, P., Kassim, M. S. M., Lazim, S. S. R. M.: Preliminary study to predict moisture content of jackfruit skin using shortwave near infrared spectroscopy. Food Research, **3**(2), 128–132 (2019).

[2] Abdullah, N.: Application of shortwave near infrared spectroscopy in determining physicochemical properties of jackfruit [Master]. Universiti Putra Malaysia (2019).

[3] Abidin, N., Ismail, S. I., Vadamalai, G., Yusof, M. T., Hakiman, M., Karam, D. S., Ismail-Suhaimy, N. W., Ibrahim, R., Zulperi, D.: Genetic diversity of Pantoea stewartii subsp. stewartii causing jackfruit-bronzing disease in Malaysia. PLOS ONE, **15**(6), e0234350 (2020). https://doi.org/10.1371/journal.pone.0234350

[4] Afonso, A. M., Antunes, M. D., Cruz, S., Cavaco, A. M., Guerra, R.: Non-destructive follow-up of 'Jintao' kiwifruit ripening through VIS-NIR spectroscopy: individual vs. average calibration model predictions. Postharvest Biology and Technology, 188, 111895 (2022). https://doi.org/10.1016/j.postharvbio.2022.111895

[5] Ali, M. M., Hashim, N., Shahamshah, M. I.: Durian (Durio zibethinus) ripeness detection using thermal imaging with multivariate analysis. Postharvest Biology and Technology, **176**, 111517 (2021). https://doi.org/10.1016/j.postharvbio.2021.111517

[6] Azad, A. K., Jones, J. G., Haq, N.: Assessing morphological and isozyme variation of jackfruit (*Artocarpus heterophyllus* Lam.) in Bangladesh. Agroforestry Systems, **71**(2), 109–125 (2007). https://doi.org/10.1007/s10457-007-9039-8

874 [7] Babu, P. S., Sudheer, K. P., Sarathjith, M. C., Mathew, S. M., Gopinath, G.: Quality evaluation
875 of tender jackfruit using near-infrared reflectance spectroscopy. Journal of Applied Horticulture,
876 **22**(3), 171–175 (2020). https://doi.org/10.37855/jah.2020.v22i03.31

877 [8] Beever, D. J.: Fruit development and fruit physiology. In: Warrington, I. J., Weston, G. C. (eds.)
878 Kiwifruit: Science and Management, pp. 97–126 (1990).

879 [9] Bharadwaj, R., Kumar, S. R., Sathishkumar, R.: Insights into role of invisible partners in plant
880 growth and development. In: Plant Growth and Stress Physiology, pp. 23–48 (2021).
881 https://doi.org/10.1007/978-3-030-78420-1_2

882 [10] Bobelyn, E., Serban, A.-S., Nicu, M., Lammertyn, J., Nicolai, B. M., Saeys, W.: Postharvest
883 quality of apple predicted by NIR spectroscopy: study of the effect of biological variability on
884 spectra and model performance. Postharvest Biology and Technology, **55**(3), 133–143 (2010).
885 https://doi.org/10.1016/j.postharvbio.2009.09.006

886 [11] Cen, H., He, Y.: Theory and application of near infrared reflectance spectroscopy in
887 determination of food quality. Trends in Food Science and Technology, **18**(2), 72–83 (2007).
888 https://doi.org/10.1016/j.tifs.2006.09.003

889 [12] Clark, C. J., McGlone, V. A., De Silva, H. N., Manning, M. A., Burdon, J., Mowat, A. D.:
890 Prediction of storage disorders of kiwifruit (Actinidia chinensis) based on visible-NIR spectral
891 characteristics at harvest. Postharvest Biology and Technology, **32**(2), 147–158 (2004).
892 https://doi.org/10.1016/j.postharvbio.2003.11.004

[13] Cozzolino, D., Cynkar, W. U., Shah, N., Smith, P.: Multivariate data analysis applied to spectroscopy: Potential application to juice and fruit quality. Food Research International, **44**(7), 1888–1896 (2011). https://doi.org/10.1016/j.foodres.2011.01.041

[14] Dadzie, B. K., Orchard, J. E.: Routine post-harvest screening of banana/plantain hybrids: criteria and methods, vol. 2. Biodiversity International (1997).

[15] Davey, M. W., Saeys, W., Hof, E., Ramon, H., Swennen, R. L., Keulemans, J.: Application of visible and near-infrared reflectance spectroscopy (Vis/NIRS) to determine carotenoid contents in banana (Musa spp.) fruit pulp. Journal of Agricultural and Food Chemistry, **57**(5), 1742–1751 (2009). https://doi.org/10.1021/jf803137d

[16] de Belie, N., Pedersen, D. K., Martens, M., Bro, R., Munck, L., De Baerdemaeker, J.: The use of visible and near-infrared reflectance measurements to assess sensory changes in carrot texture and sweetness during heat treatment. Biosystems Engineering, 85(2), 213–225 (2003). https://doi.org/10.1016/S1537-5110(03)00047-3

[17] de Oliveira, G. A., Bureau, S., Renard, C. M.-G. C., Pereira-Netto, A. B., de Castilhos, F.: Comparison of NIRS approach for prediction of internal quality traits in three fruit species. Food Chemistry, 143, 223–230 (2014). https://doi.org/10.1016/j.foodchem.2013.07.122

[18] Dias, C., Brandão, T. R., Cassoni, C., Vasconcelos, M. W., Ferrante, A., Pintado, M.: Firmness prediction of 'Rocha' pear based on non-destructive methods and shelf-life using PLS-regression modeling. Postharvest Biology and Technology, **205**, 112493 (2023). https://doi.org/10.1016/j.postharvbio.2023.112493

913 [19] Fraser, D. G., Jordan, R. B., Künnemeyer, R., McGlone, V. A.: Light distribution inside
914 mandarin fruit during internal quality assessment by NIR spectroscopy. Postharvest Biology and
915 Technology, **27**(2), 139–145 (2003). https://doi.org/10.1016/S0925-5214(02)00058-3

916 [20] Gapasin, R. M., Garcia, R. P., Advincula, C. T., De la Cruz, C. S., Borines, L. M.: Fruit
917 bronzing, a new disease affecting jackfruit caused by *Pantoea stewartii*. Annals of Tropical
918 Research, **36**(1), 17–31 (2014). https://doi.org/10.32945/atr3612.2014

919 [21] Giovanelli, G., Sinelli, N., Beghi, R., Guidetti, R., Casiraghi, E.: NIR spectroscopy for the
920 optimization of postharvest apple management. Postharvest Biology and Technology, **87**, 13–20
921 (2014). https://doi.org/10.1016/j.postharvbio.2013.07.041

922 [22] Golic, M., Walsh, K. B.: Robustness of calibration models based on near infrared
923 spectroscopy for the in-line grading of stonefruit for total soluble solids content. Analytica
924 Chimica Acta, **555**(2), 286–291 (2006). https://doi.org/10.1016/j.aca.2005.09.014

925 [23] Grabska, J., Beć, K. B., Ueno, N., Huck, C. W.: Analyzing the quality parameters of apples
926 by spectroscopy from Vis/NIR to NIR region: A comprehensive review. Foods, **12**(10), 1946
927 (2023). https://doi.org/10.3390/foods12101946

928 [24] Guthrie, J. A., Liebenberg, C. J., Walsh, K. B.: NIR model development and robustness in
929 prediction of melon fruit total soluble solids. Australian Journal of Agricultural Research, 57(4),
930 411–418 (2006). https://doi.org/10.1071/AR05123

[25] Hailu, W., Bekele, T.: Quality and physio-chemical changes associated with processing and properties of fruits and vegetables. Cogent Food and Agriculture, **10**(1), 2419957 (2024). https://doi.org/10.1080/23311932.2024.2419957

[26] Ibrahim, R., Ismail-Suhaimy, N. W., Shu-Qing, T., Ismail, S. I., Abidin, N., Hakiman, M., Karam, D. S., Ahmad-Hamdani, M. S., Yusof, M. T., Zulperi, D.: Molecular characterization and phylogenetic analysis of Pantoea stewartii subsp. stewartii causing bronzing disease of jackfruit in Malaysia based on cps and hrp gene sequences. Journal of Plant Pathology, 102(1), 193–199 (2020). https://doi.org/10.1007/s42161-019-00383-7

[27] Ibrahim, R., Ismail, S. I., Ina-Salwany, M. Y., Zulperi, D.: Biology, diagnostics, pathogenomics and mitigation strategies of jackfruit-bronzing bacterium Pantoea stewartii subsp. stewartii: What do we know so far about this culprit? Horticulturae, **8**, 702 (2022). https://doi.org/10.3390/horticulturae8080702

[28] Ismail, N., Kaur, B.: Consumer preference for jackfruit varieties in Malaysia. Journal of Agribusiness Marketing, **6**, 37–51 (2013).

[29] Li, S., Zhao, Y., Wu, P., Grierson, D., Gao, L.: Ripening and rot: How ripening processes influence disease susceptibility in fleshy fruits. Journal of Integrative Plant Biology, **66**(9), 1831–1863 (2024). https://doi.org/10.1111/jipb.13739

[30] Lim, K. J., Ding, P., Nawi, N. M., Jusoh, M.: Morphological and physical characterization of bronzing-affected jackfruit (*Artocarpus heterophyllus* Lam. cv. Tekam Yellow) across maturity stages: Influence of rind and flesh attributes. Journal of Food Science, **91**(4), e71075 (2026). https://doi.org/10.1111/1750-3841.71075

[31] Lim, K. J., Ding, P., Nawi, N. M., Jusoh, M., Abdullah, N., Lazim, S. S. R. M.: Predicting the soluble solid concentration and ascorbic acid of intact jackfruit var. Tekam Yellow using visible-near-infrared spectroscopy: Comparison of rind and flesh. Food Analytical Methods, **19**(8), 218 (2026). https://doi.org/10.1007/s12161-026-03129-1

[32] Lim, K. J., Ding, P., Nawi, N. M., Jusoh, M., Khuzaimah, Z.: Comparative evaluation of hyperspectral, thermal, and near-infrared imaging systems for non-destructive prediction of fruit and vegetable quality: A review. Journal of Nondestructive Evaluation, **45**, 79 (2026). https://doi.org/10.1007/s10921-026-01376-0

[33] Lufu, R.: Transport phenomena in pomegranate fruit: Mechanisms of weight loss and control strategies [Doctoral dissertation]. Stellenbosch University (2020). http://hdl.handle.net/10019.1/108398

[34] Magwaza, L. S., Opara, U. L., Cronje, P. J. R., Landahl, S., Nieuwoudt, H. H., Mouazen, A. M., Nicolaï, B. M., Terry, L. A.: Assessment of rind quality of 'Nules Clementine' mandarin fruit during postharvest storage: 2. Robust Vis/NIRS PLS models for prediction of physico-chemical attributes. Scientia Horticulturae, **165**, 421–432 (2014). https://doi.org/10.1016/j.scienta.2013.09.050

[35] Maniwara, P., Nakano, K., Boonyakiat, D., Ohasi, S., Hiroi, M., Tohyama, T.: The use of visible and near infrared spectroscopy for evaluating passion fruit postharvest quality. Journal of Food Engineering, **143**, 33–43 (2014). https://doi.org/10.1016/j.jfoodeng.2014.06.028

[36] Mijin, S.: Flower differentiation, pollination and syncarp development of jackfruit cv. Tekam Yellow [PhD]. Universiti Putra Malaysia (2019).

973 [37] Mishra, P., Woltering, E., Brouwer, B., Hogeveen-van Echtelt, E.: Improving moisture and
974 soluble solids content prediction in pear fruit using near-infrared spectroscopy with variable
975 selection and model updating approach. Postharvest Biology and Technology, **171**, 111348 (2021).
976 https://doi.org/10.1016/j.postharvbio.2020.111348

977 [38] Mogollon, M. R., Jara, A. F., Contreras, C., Zoffoli, J. P.: Quantitative and qualitative VIS-
978 NIR models for early determination of internal browning in 'Cripps Pink' apples during cold
979 storage. Postharvest Biology and Technology, **161**, 111060 (2020).
980 https://doi.org/10.1016/j.postharvbio.2019.111060

981 [39] Nagy, A., Riczu, P., Tamas, J.: Spectral evaluation of apple fruit ripening and pigment content
982 alteration. Scientia Horticulturae, **201**, 256–264 (2016).
983 https://doi.org/10.1016/j.scienta.2016.02.016

984 [40] Nicolaï, B. M., Beullens, K., Bobelyn, E., Peirs, A., Saeys, W., Theron, K. I.: Non-destructive
985 measurement of fruit and vegetable quality by means of NIR spectroscopy: A review. Postharvest
986 Biology and Technology, **46**(2), 99–118 (2007).
987 https://doi.org/10.1016/j.postharvbio.2007.06.024

988 [41] Osborne, B. G., Fearn, T., Hindle, P. H.: Practical NIR spectroscopy with applications in food
989 and beverage analysis. Longman Scientific and Technical, Harlow (1993).

990 [42] Peng, Z., Liu, G., Li, H., Wang, Y., Gao, H., Jemrić, T., Fu, D.: Molecular and genetic events
991 determining the softening of fleshy fruits: A comprehensive review. International Journal of
992 Molecular Sciences, **23**(20), 12482 (2022). https://doi.org/10.3390/ijms232012482

[43] Peirs, A., Tirry, J., Verlinden, B., Darius, P., Nicolaï, B. M.: Effect of biological variability on the robustness of NIR models for soluble solids content of apples. Postharvest Biology and Technology, **28**(2), 269–280 (2003). https://doi.org/10.1016/S0925-5214(02)00196-5

[44] Rosli, H. G., Civello, P. M., Martínez, G. A.: Changes in cell wall composition of three Fragaria × ananassa cultivars with different softening rate during ripening. Plant Physiology and Biochemistry, **42**(10), 823–831 (2004). https://doi.org/10.1016/j.plaphy.2004.10.002

[45] Saechua, W., Sharma, S., Nakawajana, N., Leepaitoon, K., Chunsri, R., Posom, J., Pornchaloempong, P.: Integrating Vis-SWNIR spectrometer in a conveyor system for in-line measurement of dry matter content and soluble solids content of durian pulp. Postharvest Biology and Technology, **181**, 111640 (2021). https://doi.org/10.1016/j.postharvbio.2021.111640

[46] Saeys, W., Mouazen, A. M., Ramon, H.: Potential for onsite and online analysis of pig manure using visible and near infrared reflectance spectroscopy. Biosystems Engineering, **91**(4), 393–402 (2005). https://doi.org/10.1016/j.biosystemseng.2005.05.001

[47] Saxena, A., Bawa, A. S., Raju, P. S.: Jackfruit (*Artocarpus heterophyllus* Lam.). In: Postharvest Biology and Technology of Tropical and Subtropical Fruits, pp. 275–299 (2011). https://doi.org/10.1533/9780857092885.275

[48] Sirisomboon, P., Boonmung, S., Pornchaloempong, P., Pithuncharurnlap, M.: A preliminary study on classification of mango maturity by compression test. International Journal of Food Properties, **11**(1), 206–212 (2008). https://doi.org/10.1080/10942910701435430

[49] Smolikova, G., Leonova, T., Vashurina, N., Frolov, A., Medvedev, S.: Desiccation tolerance as the basis of long-term seed viability. International Journal of Molecular Sciences, **22**(1), 101 (2020). https://doi.org/10.3390/ijms22010101

[50] Tortorella, I., Argentati, C., Emiliani, C., Morena, F., Martino, S.: Biochemical pathways of cellular mechanosensing/mechanotransduction and their role in neurodegenerative diseases pathogenesis. Cells, **11**(19), 3093 (2022). https://doi.org/10.3390/cells11193093

[51] Wang, S., Yan, J., Tian, S., Tian, H., Xu, H.: Vis/NIR model development and robustness in prediction of potato dry matter content with influence of cultivar and season. Postharvest Biology and Technology, 197, 112202 (2023). https://doi.org/10.1016/j.postharvbio.2022.112202

[52] Wang, Y. D., Veltkamp, D. J., Kowalski, B. R.: Multivariate instrument standardization. Analytical Chemistry, **63**(23), 2750–2756 (1991). https://doi.org/10.1021/ac00023a016

[53] Workman, J. J.: A review of calibration transfer practices and instrument differences in spectroscopy. Applied Spectroscopy, **72**(3), 340–365 (2018). https://doi.org/10.1177/0003702817736064

[54] Zulperi, D., Manaf, N., Ismail, S. I., Karam, D. S., Yusof, M. T.: First report of *Pantoea stewartii* subsp. *stewartii* causing fruit bronzing of jackfruit (*Artocarpus heterophyllus*), a new emerging disease in Peninsular Malaysia. Plant Disease, **101**(5), 831 (2017). https://doi.org/10.1094/PDIS-11-16-1689-PDN